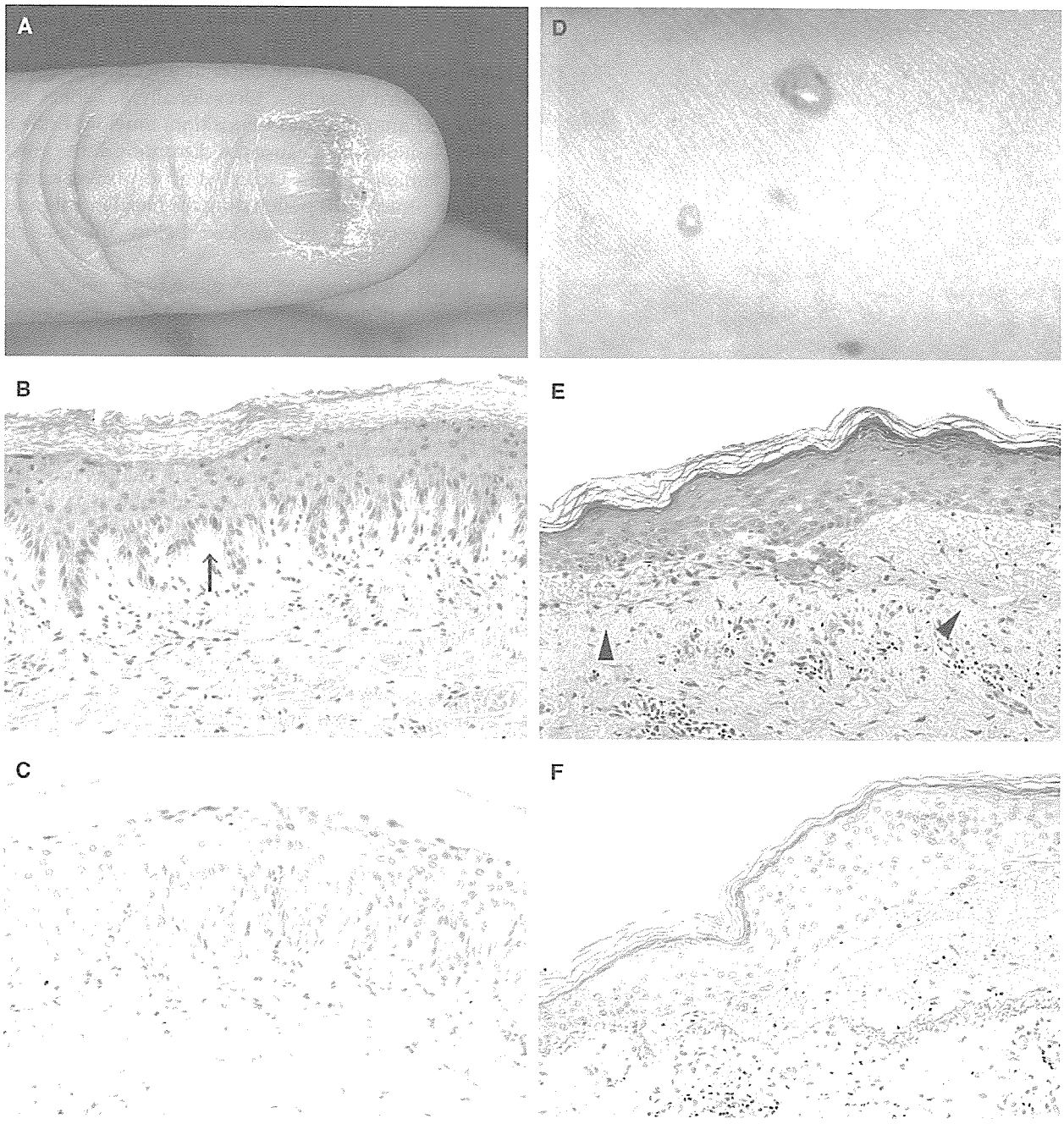

Fig 1. Clinical features and histopathologic findings. **A**, Brittleness, longitudinal ridging and lamellar splitting of the nail plates were seen on fingernails. **B**, Biopsy specimen from nail bed of patient's right forefinger demonstrated mild eosinophilic deposits within dermal papilla *(arrow)*. **C**, Direct fast scarlet staining showed orange amyloid deposits clearly. **D**, Tense bullae, easily induced by mechanical stimuli, were observed on forearms. **E**, Biopsy specimen from blister on forearm revealed subepidermal separation and eosinophilic deposits *(arrowheads)* on superficial dermis. **F**, Orange deposits were observed beneath bulla and dermal papilla, resistant to potassium-permanganate. (**B** and **E**, Hematoxylin-eosin stain; **C** and **F**, direct fast scarlet stain; original magnification: **B**, **C**, **E**, **F**, ×40.)

Electron microscopy demonstrated amorphous deposits without clefts beneath the basal membrane, not within the lamina lucida. The deposition consisted of straight amyloid fibrils, linking the blisters with the underlying systemic amyloidosis. The patient died of exacerbated multiple myeloma 3 months after the initial blister formation.

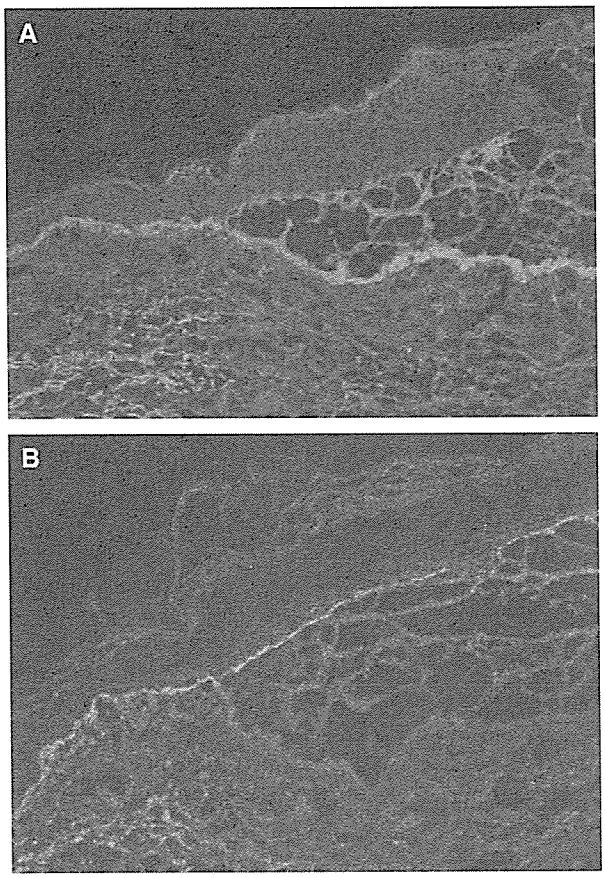

Fig 2. Fluorescence antigen mapping. **A**, Antibody directed against type IV collagen (CIV22) mapped to bottom of bulla. **B**, On top of bulla, antibody against β_4 integrin (3E1) was noted at separation of blister roof. (**A** and **B**, original magnification ×40.)

DISCUSSION

Nail dystrophy is a rare symptom of systemic amyloidosis and usually manifests as brittleness, longitudinal ridging and splitting. It may be the initial mucocutaneous manifestation[1,2] and tends to slowly worsen over the course of several years.[2-4] Occasionally, nail changes represent the sole cutaneous sign of systemic amyloidosis.[4]

Bullous amyloidosis is caused by local amyloid deposition resulting in cutaneous blisters. This is a rare finding. Bullae may appear at any time during the course of disease but tend to progress over a period of years. A site of predilection is the skin folds, where blisters form after mild mechanical friction (Nikolskiy sign), as in our case.[5,6] The exact pathogenesis of this phenomenon is unknown.

Several possible mechanisms of blister formation have been reported. Clefts may originate at the site of significant amyloid deposition in the dermis, resulting in dermal blisters.[5,7] Occasionally, no splits are observed after amyloid deposition; amyloid bodies below lamina densa cause the disruption at the level of the lamida lucida.[8] Ochiai et al[9] observed keratinocyte protrusions penetrating the basal membrane and surrounding the amyloid below the lamina densa.

In this case, amyloid deposits were noted below the basement membrane using electron microscopy, and blisters formed within the lamina lucida were detected by fluorescence antigen mapping. No apparent keratinocyte protrusions were observed. We believe that these bullae could be caused by basement membrane fragility resulting from amyloid deposition just below lamina densa, leading to splits in the lamina lucida, the most vulnerable part of the basement membrane.

This case demonstrates the rare mucocutaneous manifestations of nail dystrophy and bullous amyloidosis, the latter caused by blister formation within the lamina lucida. It serves as a reminder that these unusual cutaneous phenomena may represent important diagnostic signs of systemic amyloidosis, even without other appreciable mucocutaneous or visceral involvement.

We thank Dr James R. McMillan for his critical proofreading of this manuscript.

REFERENCES

1. Breathnach SM. Amyloid and amyloidosis. J Am Acad Dermatol 1988;18:1-16.
2. Fanti PA, Tosti A, Morelli R, Galbiati G. Nail changes as the first sign of systemic amyloidosis. Dermatologica 1991;183:44-6.
3. Ostlere LS, Stevens H, Mehta A, Rustin MH. Nail dystrophy. Arch Dermatol 1995;131:953, 956.
4. Mancuso G, Fanti PA, Berdondini RM. Nail changes as the only skin abnormality in myeloma-associated systemic amyloidosis. Br J Dermatol 1997;137:471-2.
5. Robert C, Aractingi S, Prost C, Verola O, Blanchet-Bardon C, Blanc F, et al. Bullous amyloidosis: report of 3 cases and review of the literature. Medicine (Baltimore) 1993;72:38-44.
6. Houman MH, Smiti Khanfir M, Ben Ghorbel I, Mokni M, Jerbi E, Boubaker S, et al. [Bullous amyloidosis.] Ann Dermatol Venereol 2002;129:299-302. French.
7. Bluhm JF, Johnson SC, Norback DH. Bullous amyloidosis: case report with ultrastructural studies. Arch Dermatol 1980;116: 1164-8.
8. Ruzicka T, Schmoeckel C, Ring J, Linke RP, Braun-Falco O. Bullous amyloidosis. Br J Dermatol 1985;113:85-95.
9. Ochiai T, Morishima T, Hao T, Takayama A. Bullous amyloidosis: the mechanism of blister formation revealed by electron microscopy. J Cutan Pathol 2001;28:407-11.

Mod Rheumatol (2006) 16:229–234
DOI 10.1007/s10165-006-0496-0

ORIGINAL ARTICLE

Makoto Goto · Masako Okawa-Takatsuji
Shinichi Aotsuka · Hidenori Nakai · Masatosi Shimizu
Hideyuki Goto · Akira Shimamoto · Yasuhiro Furuichi

Significant elevation of IgG anti-WRN (RecQ3 RNA/DNA helicase) antibody in systemic sclerosis

Received: April 5, 2006 / Accepted: May 22, 2006

Abstract Werner syndrome, caused by the homologous mutation of RecQ3 RNA/DNA helicase (WRN), is often misdiagnosed as systemic sclerosis (SSc) because of apparent similar skin changes and its relatively high frequency in Japan. The present study was undertaken to determine whether anti-WRN antibodies assayed by specific enzyme-linked immunosorbent assay occur in 41 SSc patients (30 diffuse and 11 limited types) and, if so, to determine any clinical association, such as skin sclerosis. Serum level of IgG anti-WRN antibody in SSc was significantly higher than that from 30 age- and sex-matched normal volunteers ($P < 0.001$). The serum level of IgG anti-WRN antibody in diffuse type SSc was significantly higher than the limited type ($P < 0.05$). A significant correlation was observed between serum levels of IgG anti-topoisomerase I antibody and IgG anti-WRN antibody in the same samples from SSc ($P < 0.05$). Moreover, in 119 normal healthy individuals aged from 0 to 99 years, a statistically significant correlation ($P < 0.001$) existed between serum level of IgG anti-WRN antibody and advancing age. A significantly higher level of IgG autoantibody specific for WRN detected in diffuse than in limited type SSc and normal may contribute to the pathogenesis of skin sclerosis in SSc.

M. Goto (✉)
Division of Anti-Ageing and Longevity Sciences, Department of Clinical Engineering, Faculty of BioMedical Engineering, Toin University of Yokohama, 1614 Kurogane-cho, Aoba-ku, Yokohama 225-8502, Japan
Tel./Fax +81-45-974-5132
e-mail: goto@cc.toin.ac.jp

M. Okawa-Takatsuji · S. Aotsuka
Department of Clinical Immunology, International Medical Center of Japan, Tokyo, Japan

H. Nakai
Department of Internal Medicine, Kinnikyo Sapporo Hospital, Sapporo, Japan

M. Shimizu
Division of Rheumatology, Hino Hospital, Hino, Japan

H. Goto · A. Shimamoto · Y. Furuichi
GeneCare Research Institute, Kamakura, Japan

Key words Aging · Anti-helicase antibody · DNA metabolism · Systemic sclerosis (SSc) · Werner syndrome

Introduction

Systemic skin sclerosis is the hallmark of both systemic sclerosis (SSc) and Werner syndrome (WS; MIM #27770). Werner syndrome, caused by the homologous mutation of RecQ3 RNA/DNA helicase (WRN), is an autosomal recessively inherited disease with progeroid phenotypes.[1–5] Patients with WS manifest a series of accelerated forms of normal aging phenotypes after an early termination of teenage growth spurt followed by gray hair, alopecia, juvenile cataract, voice change, skin atrophy, skin sclerosis, telangiectasia, skin hyper-/hypopigmentation, skin ulcers, osteoporosis, hypogonadism, diabetes mellitus, atherosclerosis, subcutaneous calcification, brain atrophy, and malignant tumors, followed by death before 50 years of age.[1,2] They also manifest a mild lung fibrosis, sclerodactyly, and in some limited cases sicca syndrome, thyroid diseases, arthritis, and systemic lupus erythematosus, but have never shown an esophageal dilatation, Raynaud phenomenon, or pulmonary hypertension.[1,6] As a whole, patients with WS mimic an accelerated form of natural aging and thus WS has been selected as a top-ranking model of human aging.

Helicases are RNA/DNA metabolism enzymes with the common function of unwinding of the helical structure of double-stranded RNA/DNA to single strands.[7] RecQ3 RNA/DNA helicase (WRN) was believed to function in the nucleolus within the nucleus.[8,9] The DNA enzyme; topoisomerase I, whose antibody (anti-topoisomerase I: Scl-70) is the specific disease marker antibody for SSc, colocalizes and seems to work in association with RecQ3 RNA/DNA helicase in cases of RNA/DNA metabolism such as repair, replication, recombination, and transcription.[10–12] The nucleolar pattern of fluorescent antinuclear antibody was usually detected in the sera from SSc.[12] As the frequency of WS in Japan is extremely high compared with elsewhere[1,5] as well as clinically similar skin changes such as

Table 1. Demography of the patients with systemic sclerosis

		Diffuse	Limited	Normal volunteer
No. of patients		30 (F 27, M 3)	11 (F 11)	30 (F 28, M 2)
Age (years)	Mean ± SD	47.7 ± 13.8	51.7 ± 17.0	48.2 ± 15.3
	Range	23–72	17–72	24–70
Disease duration (years)	Mean ± SD	11.4 ± 8.6	8.6 ± 8.1	–
	Range	1–32	2–30	–
Therapy (%)	Prednisolone (<10 mg)	43.3	36.4	–
	D-Penicillamine	26.7	36.4	–
	PGI_2	10	0	–
	Calcium channel blocker	7	9.1	–
	None	20	18.1	–

PGI_2, prostacyclin

scleroderma, hyper/hypopigmentation, telangiectasia, skin ulcer, and subcutaneous calcification between WS and SSc, we studied the possible contribution of anti-WRN autoantobodies to the pathogenesis of skin sclerosis in SSc.

Patients and methods

Patients

Sera from a total of 41 patients with SSc who met the American College of Rheumatology (formerly, American Rheumatism Association) preliminary classification criteria for SSc[13] and 119 apparently healthy normal individuals of both sexes aged from 0 to 99 years were collected and stored at –70°C until use. In comparing the difference of antibody levels between SSc and normal, 30 age- and sex-matched healthy normal volunteers among the healthy individuals were selected as the control. The demographic data of the patients are summarized in Table 1. Basically, no significant difference was found between the patients with diffuse type SSc and limited type SSc in terms of age, disease duration, and type of therapy. The Institutional Review Board of Toin University, Yokohama approved the study.

Preparation of RecQ3 RNA/DNA helicase (WRN) protein and anti-WRN antibody

Cloning and purification of WRN protein and the preparation of anti-WRN antibody were described previously.[14,15] The purity of the recombinant WRN protein was ~80% determined by CBB staining.

Immunoblotting for the detection of anti-WRN antibody

Immunoblot analysis for autoantibody against RecQ3 RNA/DNA helicase was performed as follows. Recombinant RecQ3RNA/DNA helicase was electrophoresed on 2%–15% sodium dodecyl sulfate–polyacrylamide gel electrophoresis gel and electroblotted to a nitrocellulose sheet. After blocking with bovine serum albumin/Tris–HCl buffer, 1:50 diluted SSc serum was incubated with the nitrocellulose sheet. After washing, 1:1000 diluted alkaline phosphatase-conjugated antihuman IgG antibody was added and incubated. The sheet was washed with the buffer, incubated with the substrate solution, and then washed thoroughly with deionized water.

Enzyme-linked immunosorbent assay (ELISA) for antibody binding to RecQ3 RNA/DNA helicase

Polystyrene microtiter plates were coated with 100 µl WRN protein (10 µl/ml in Tris–HCl buffer, pH 7.6) by overnight incubation at 4°C. After blocking with 300 µl 1% bovine serum albumin (BSA) in Tris–HCl buffer for 30 min, sera were diluted 1:100 and incubated overnight at 4°C in duplicate WRN-coated wells and duplicate BSA-coated wells. Bound antibody was detected with horseradish peroxidase (HRP)-conjugated goat anti-human IgG or IgM antibody (1:2000). The peroxidase substrate *ortho*-phenylenediamine and H_2O_2 was used as chromagen. Absorbance at 490 nm (A_{490}) was measured using an automated spectrophotometer as described previously.[16] The binding activities of the antibody are expressed as an index calculated by the following formula: Index = [sample (A_{490})–negative control (A_{490})] × 100/[positive control (A_{490})–negative control (A_{490})]. The serum with the highest anti-WRN antibody level was arbitrarily set as positive control (Index = 200).

Inhibition assay

The capacity of WRN protein to block antibody binding in the representative sera to solid-phase WRN protein was measured by adding increasing amounts of WRN protein (~40 µg/ml) to the sera with elevated IgG anti-WRN activity. The final serum concentration was 1:100, and the

incubation time at room temperature was 60 min. The residual IgG antibody-binding capacity to solid-bound WRN protein was determined by ELISA as described above.

ELISA for anti-topoisomerase I antibody

Serum IgG autoantibody against topoisomerase I (Scl-70) was measured by using a commercially available ELISA kit (MESACUP-2 test Scl-70; MBL, Nagoya, Japan). The data were expressed according to the manufacturer's suggestion.

Statistical analysis

Data are given as the mean and 2 standard deviations (mean±2 SD) or the median and interquartile range. Data analyses were performed using a statistical analysis software package (StatFlex; ViewFlex, Tokyo, Japan) to evaluate the Mann–Whitney *U*-test and Pearson's correlation test. Differences with *P* values less than 0.05 were considered to be statistically significant.

Results

Serum levels of anti-RecQ3 RNA/DNA helicase (WRN) in SSc

The median and interquartile (Q1–Q3) serum level of IgG anti-WRN antibody in the patients with SSc (131.2 and 89.1–170.0 Index, $n = 41$) was significantly higher than that in age- and sex-matched normal volunteers (71.2 and 58.0–105.5 Index, $n = 30$, $P < 0.001$, Wilcoxon *t*-test, Fig. 1a). The median and interquartile serum level of IgM anti-WRN antibody in the patients with SSc (79.4 and 51.1–111.7 Index, $n = 41$) was also significantly higher than that in age- and sex-matched normal volunteers (55.7 and 38.3–71.3 Index, $n = 30$, $P < 0.05$, Fig. 1b). Moreover, the median and interquartile serum level of IgG anti-WRN antibody in the patients with SSc of diffuse type (142.9 and 118.1–184.1 Index, $n = 30$) was significantly higher than that of limited type (92.7 and 80.1–97.2 Index, $n = 11$, $P < 0.01$, Fig. 2). Cutoff value for the positivity of IgG anti-WRN was arbitrarily settled based on the mean±2 SD (56.2 ± 30.6 = 86.8 Index) from normal volunteers ages between 20 and 60. Positive serum for IgG anti-WRN was 80% in diffuse type SSc, while less than 10% serum was IgG anti-WRN positive in limited type SSc and normal volunteers. Neither a significant correlation between IgG, IgM, or IgA anti-WRN antibody in the SSc sera with disease duration, patients' age, sex, clinical phenotypes other than scleroderma, nor type of therapy was observed (data not shown).

Relationship between serum levels of IgG anti-WRN and IgG anti-topoisomerase I antibody

A significant correlation was observed between serum levels of igG anti-WRN and anti-topoismerase I antibodies in the patients with SSc ($r = 0.363$, $n = 41$, $P < 0.05$; Fig. 3).

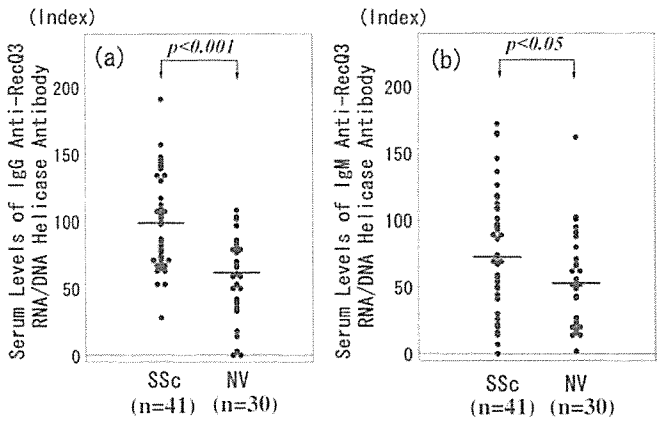

Fig. 1a,b. Anti-RecQ3 RNA/DNA helicase antibodies (anti-WRN) in systemic sclerosis (*SSc*). Serum levels of IgG (**a**) and IgM (**b**) anti-WRN in the patients with SSc ($n = 41$) were compared with those from age- and sex-matched normal volunteers (*NV*; $n = 30$). **a** The median (indicated by *bars*) serum level of IgG anti-WRN in SSc was 131.2 Index, while that of normal volunteers was 71.2 Index ($P < 0.001$). **b** The median serum levels of IgM anti-WRN in SSc were 79.4 Index and 55.7 Index in normal volunteers. The difference was also significant ($P < 0.05$)

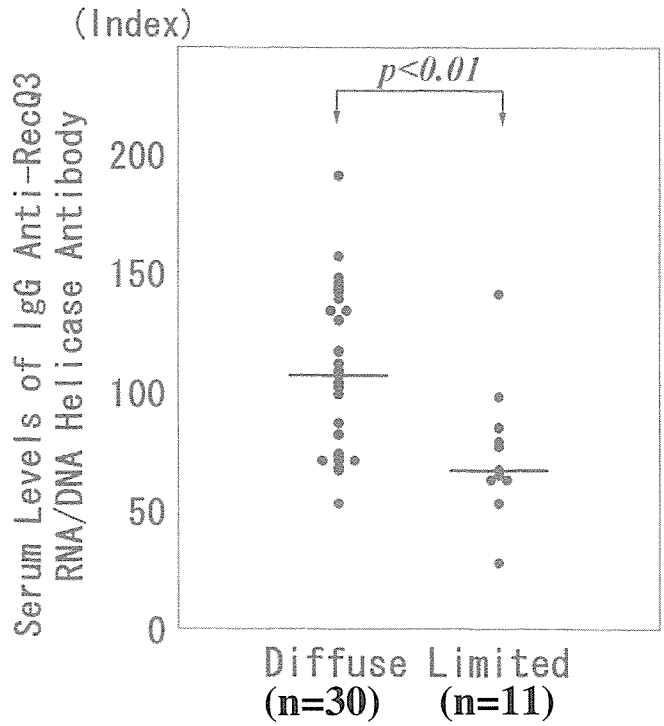

Fig. 2. Serum level of IgG anti-WRN in SSc of diffuse type and limited type. The median serum level of IgG anti-WRN in diffuse type SSc ($n = 30$) was 142.9 Index, while that of limited type SSc ($n = 11$) was 92.7. The difference was statistically significant ($P < 0.01$)

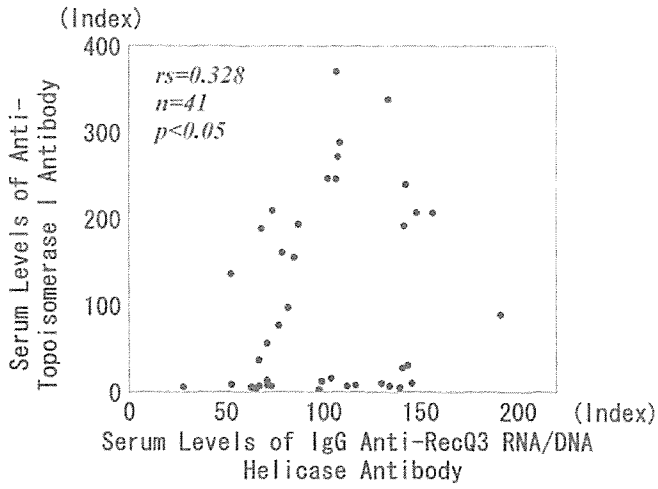

Fig. 3. Relationship between serum levels of IgG anti-WRN and anti-topoisomerase I antibody in patients with SSc. If the relationship between the IgG levels of anti-WRN and anti-topoisomerase I antibodies was examined in the same sera from SSc, a statistically significant correlation ($P < 0.05$) was observed

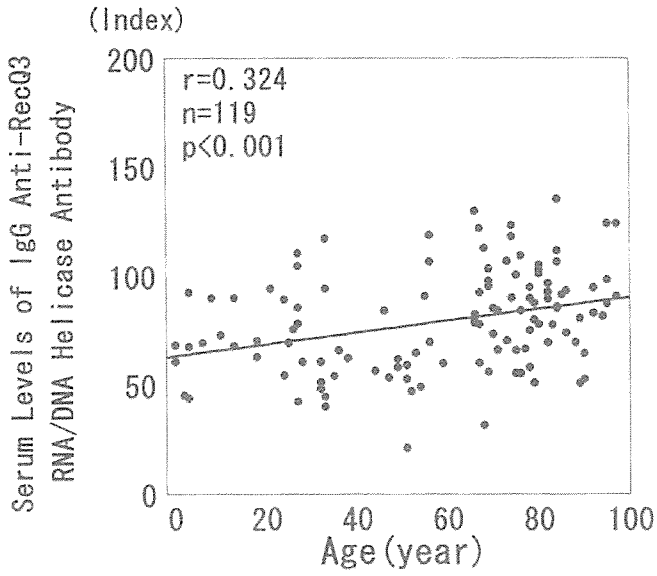

Fig. 4. Correlation between age and serum level of IgG anti-WRN in normal individuals. Age dependency of the serum IgG anti-WRN level among healthy individuals from 0 to 99 years old was significant ($P < 0.001$)

Serum level of IgG anti-WRN changes with age in the healthy population

In the 119 normal healthy individuals aged from 0 to 99 years, serum level of anti-WRN of IgG type correlated significantly with advancing age ($P < 0.001$) as depicted in Fig. 4. Serial analysis of IgG anti-WRN antibody in the same individuals for several years showed relatively constant levels (data not shown).

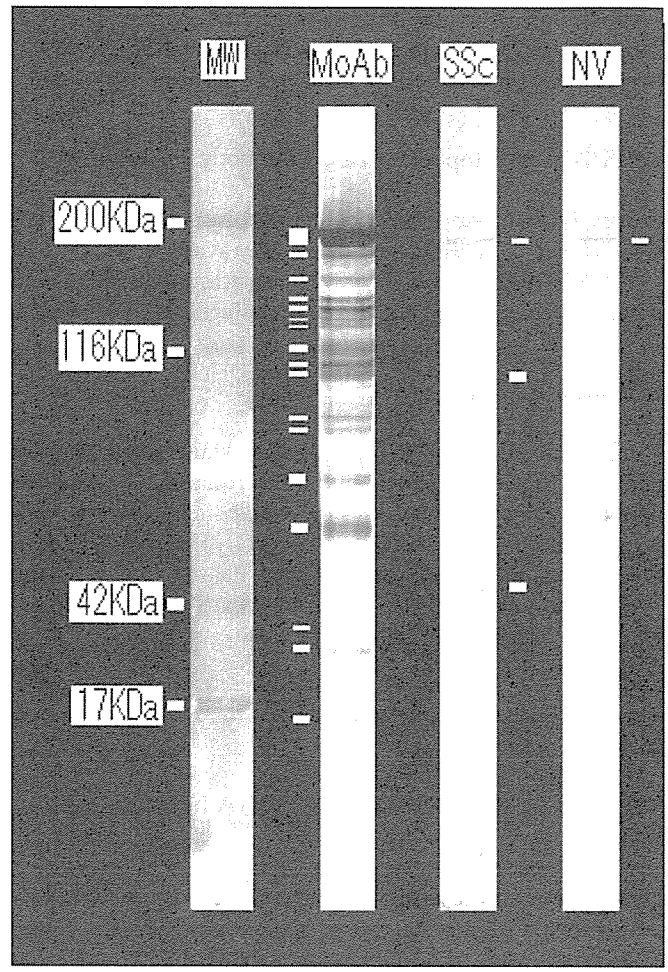

Fig. 5. Immunoblot analysis for reactivity of SSc serum with recombinant RecQ3 RNA/DNA helicase. Western blotting experiment showed a 200-kDa band specific to RecQ3 RNA/DNA helicase. *MW*, molecular weight marker; *MoAb*, monoclonal antibody against recombinant RecQ3 RNA/DNA helicase; *SSc*, systemic sclerosis; *NV*, normal volunteers

Specificity of the antibody to RecQ3 RNA/DNA helicase (WRN)

Western blotting showed a 200-kDa specific band of anti-WRN autoantibody from both SSc patients and normal volunteers to the recombinant WRN protein (Fig. 5). Inhibition of the specific binding capacity of anti-WRN antibody in the representative sera from both SSc patients and normal volunteers was observed by adding increasing amounts of recombinant WRN protein in a similar fashion, as shown in Fig. 6.

Discussion

Both SSc and WS have similar skin changes, i.e., scleroderma, hyper-/hypopigmentation, telangiectasia, skin ulcers, painful corns, and subcutaneous calcification, in addition to generalized fibrosis, though SSc has been believed

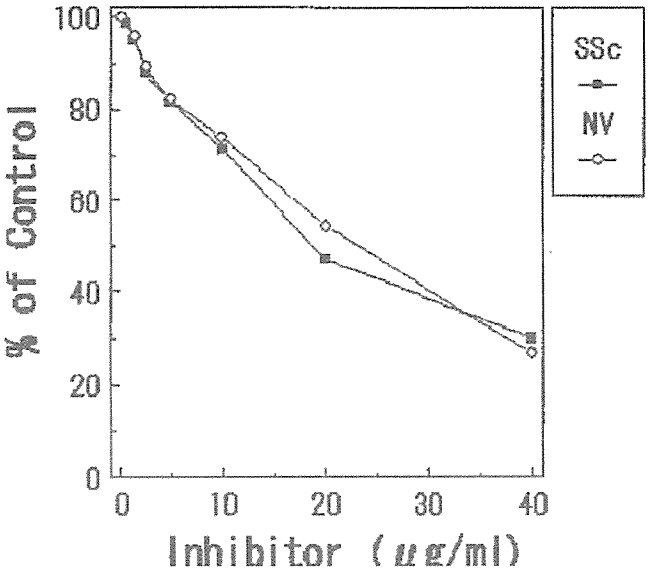

Fig. 6. Inhibition of IgG anti-WRN (RecQ3 RNA/DNA helicase antibody by RecQ3 RNA/DNA helicase protein. The sera from the representative SSc patient and a normal volunteer were incubated with an increasing amount (0–40 μg/ml) of recombinant RecQ3 RNA/DNA helicase protein at room temperature for 60 min. The residual IgG anti-RecQ3 RNA/DNA helicase antibody level was determined by the specific enzyme-linked immunosorbent assay. Inhibition of the specific binding of IgG anti-RecQ3 RNA/DNA helicase (WRN) of the SSc patients and normal volunteers to solid-phase coated recombinant RecQ3 RNA/DNA helicase protein was expressed as percent of control. Similar results were obtained using other SSc samples

to be the result of unidentified autoimmune mechanisms in contrast to the autosomal-recessively inherited WS caused by the loss of function of the mutated RecQ3 RNA/DNA helicase (WRN). We have been exploring common mechanisms in terms of connective tissue metabolism underlying between WS and SSs.[1] We have demonstrated for the first time that IgG autoantibody to a nucleolar RecQ3 RNA/DNA helicase (WRN) protein occurs in 80% of patients with diffuse type SSc, and may be associated with systemic skin sclerosis in SSc (Figs. 1 and 2). The presence of anti-WRN antibodies, however, is not specific for SSc, since positive serum was found in a separate experiment from other autoimmune diseases including systemic lupus erythematosus, rheumatoid arthritis, Sjögren syndrome, mixed connective tissue disease, and even aged normal individuals, though both the frequency and the titer are relatively low.

Systemic sclerosis is a relatively uncommon human disease characterized by progressive fibrosis of the skin and internal organs, including the lungs and gastrointestinal tract, with unknown etiology. Most scientists believe an inciting immunologic imbalance to be the primary cause of the disease, like other autoimmune diseases, but despite much research over the past half century, the underlying mechanisms remain unclear. One important clue to its etiology is the nearly universal association of disease with autoantibodies, which are antibodies directed against ubiquitous host proteins (autoantigens) such as topoisomearase I. RecQ3 RNA/DNA helicase is also a ubiquitous protein and functions in accordance with other enzymes such as topoisomearase I, II, and III, Ku, proliferating cell nuclear antigen, RNA polymerase I, II, and III in RNA/DNA metabolism.[8,17] The autoantibodies against these RNA/DNA enzymes are frequently detected in autoimmune diseases including SSc, though we still do not know whether their autoantibodies detected in the circulation are merely the byproduct of normal apoptosis or diseased damage and have something to do with etiology, or have any pathogenetic role in the autoimmune diseases. Some autoantibody has been shown to have a nuclear localization signal and may intrude into the nucleus, suggesting a possible coordination with RNA/DNA enzymes within the nucleus or nucleolus,[18,19] though we do not know if the IgG anti-WRN antibody has the nuclear localization signal or has a binding capacity to the cell membrane of fibroblasts in SSc like anti-topoisomearase I antibody, as reported previously.[20]

The role of IgG anti-WRN autoantibody in the pathogenesis of skin sclerosis is not clear. Elevated serum IgG is frequently detected in patients with SSc and aged individuals and may share common mechanisms with the production of IgG anti-WRN autoantibody. We would like to speculate a role of IgG anti-WRN in the skin atrophy followed by skin sclerosis tightly associated with the normal aging process and SSc.

Acknowledgments A part of this study was presented as a poster at the 2005 Annual Scientific Meeting of the ACR held in San Diego, CA, USA. This study was supported in part by a 2001 Novartis Rheumatology Award (M.G.).

References

1. Goto M. Werner syndrome: from clinics to genetics. Exp Rheumatol 2000;18:760–6.
2. Goto M. Clinical characteristics of Werner syndrome and other premature aging syndromes: pattern of aging in progeroid syndromes. In: Goto M, Miller RW, editors. From premature gray hair to helicase – Werner syndrome: implications for aging and cancer. Basel: Karger; 2001. p. 27–39.
3. Masuda T, Akasaka Y, Ito K, Ishikawa Y, Ishii T. Pathology: Werner syndrome and normal aging. In: Goto M, Miller RW, editors. From premature gray hair to helicase – Werner syndrome: implications for aging and cancer. Basel: Karger; 2001. p. 41–50.
4. Hatamochi A. Dermatological features and collagen metabolism in Werner syndrome. In: Goto M, Miller RW, editors. From premature gray hair to helicase – Werner syndrome: implications for aging and cancer. Basel: Karger; 2001. p. 51–9.
5. Satoh M, Matsumoto T, Imai M, Tsugane S, Furuichi Y, Goto M. Prevalence of Werner syndrome gene mutations in the Japanese population: a genetic epidemiological study. In: Goto M, Miller RW, editors. From premature gray hair to helicase – Werner syndrome: implications for aging and cancer. Basel: Karger; 2001. p. 19–25.
6. Kogure A, Ohshima N, Watanabe N, Ohba T, Miyata M, Ohara M, et al. A case of Werner's syndrome associated with systemic lupus erythematosus. Clin Rheumatol 1995;14:199–203.
7. van Brabant AJ, Stan R, Ellis NA. DNA helicases, genomic instability, and human genetic disease. Annu Rev Genomics Hum Genet 2000;1:409–59.
8. Oshima J. Functions of WRN helicase protein. In: Goto M, Miller RW, editors. From premature gray hair to helicase – Werner syndrome: implications for aging and cancer. Basel: Karger; 2001. p. 125–35.

9. Matsumoto T, Imamura O, Goto M, Furuichi Y. Characterization of the nuclear localization signal in the DNA helicase involved in Werner's syndrome. Int J Mol Med 1998;1:71–6.
10. Shero JH, Bordwell B, Rothfield NF, Earnshaw WC. High titers of autoantibodies to topoisomerase I(Scl-70) in sera from scleroderma patients. Science 1986;231:737–40.
11. Wang JC. DNA topoisomerases. Annu Rev Biochem 1985;54:665–97.
12. Lebel M, Spillare EA, Harris CC, Leder P. The Werner syndrome gene product co-purifies with the DNA replication complex and interacts with PCNA and topoisomerase I. J Biol Chem 1999;274:37795–99.
13. Subcommittee for Scleroderma Criteria of the American Rheumatism Association Diagnostic and Therapeutic Criteria Committee. Preliminary criteria for the classification of systemic sclerosis (scleroderma). Arthritis Rheum 1980;23:581–90.
14. Suzuki N, Shimamoto A, Kuromitsu J, Goto M, Furuichi Y. DNA helicase activity in Werner's syndrome gene product synthesized in a baculovirus system. Nucleic Acids Res 1997;25:2973–8.
15. Shiratori M, Sakamoto S, Suzuki N, Enomoto T, Sugimoto M, Goto M, et al. Detection by epitope-defined monoclonal antibodies of Werner DNA helicases in the nucleoplasm and their upregulation by cell transformation and immortalization. J Cell Biol 1999;144:1–9.
16. Minatani M, Aotsuka S, Satoh T. Autoantibodies against C-reactive protein (CRP) in sera of patients with systemic rheumatic diseases. Mod Rheumatol 1991;11:127–31.
17. Branzei D, Enomoto T. Proteins that interact with the Werner syndrome gene product. In: Lebel M, editor. Molecular mechanisms of Werner's syndrome. Georgetown: Landes Bioscience/Eurekah.Com; 2003. p. 44–61.
18. Yaoita Y, Takahashi M, Azuma C, Kanai Y, Honjo T. Biased expression of variable region gene families of the immunoglobulin heavy chain in autoimmune-prone mice. J Biochem (Tokyo) 1988;104:337–43.
19. Panosiou-Sahakian N, Klotz JL, Fbling F, Kronenberg M, Hahn B. Diversity of Ig V gene segments found in anti-DNA autoantibodies from a single (NZB×NZW) F1 mouse. J Immunol 1989;142:4500–6.
20. Henault J, Tremblay M, Clement I, Raymond Y, Senecal JL. Direct binding of anti-DNA topoisomerase I autoantibodies to the cell surface of fibroblasts in patients with systemic sclerosis. Arthritis Rheum 2004;50:3265–74.

ORIGINAL ARTICLE

See related commentary on page 708

Fibroblasts Show More Potential as Target Cells than Keratinocytes in *COL7A1* Gene Therapy of Dystrophic Epidermolysis Bullosa

Maki Goto[1], Daisuke Sawamura[1], Kei Ito[1], Masataka Abe[1], Wataru Nishie[1], Kaori Sakai[1], Akihiko Shibaki[1], Masashi Akiyama[1] and Hiroshi Shimizu[1]

Dystrophic epidermolysis bullosa (DEB) is an inherited blistering skin disorder caused by mutations in the type VII collagen gene (*COL7A1*). Therapeutic introduction of *COL7A1* into skin cells holds significant promise for the treatment of DEB. The purpose of this study was to establish an efficient retroviral transfer method for *COL7A1* into DEB epidermal keratinocytes and dermal fibroblasts, and to determine which gene-transferred cells can most efficiently express collagen VII in the skin. We demonstrated that gene transfer using a combination of G protein of vesicular stomatitis virus-pseudotyped retroviral vector and retronectin introduced *COL7A1* into keratinocytes and fibroblasts from a DEB patient with the lack of *COL7A1* expression. Real-time polymerase chain reaction analysis of the normal human skin demonstrated that the quantity of *COL7A1* expression in the epidermis was significantly higher than that in the dermis. Subsequently, we have produced skin grafts with the gene-transferred or untreated DEB keratinocytes and fibroblasts, and have transplanted them into nude rats. Interestingly, the series of skin graft experiments showed that the gene-transferred fibroblasts supplied higher amount of collagen VII to the new dermal–epidermal junction than the gene-transferred keratinocytes. An ultrastructural study revealed that collagen VII from gene-transferred cells formed proper anchoring fibrils. These results suggest that fibroblasts may be a better gene therapy target of DEB treatment than keratinocytes.

Journal of Investigative Dermatology (2006) **126,** 766–772. doi:10.1038/sj.jid.5700117; published online 26 January 2006

INTRODUCTION

Type VII collagen, a non-fibrillar collagen, is a major component of anchoring fibril loop structures beneath the epidermal basement membrane (Uitto *et al.*, 1992; Burgeson, 1993). Cloning of collagen VII cDNA demonstrated a primary sequence of 2,944 amino acids and the basic organization of the functional domains (Christiano *et al.*, 1994a). Subsequent genomic cloning has highlighted the structural organization of the collagen VII gene (*COL7A1*) (Christiano *et al.*, 1994b). This cloning information has enabled genomic DNA sequence analysis of *COL7A1* and has demonstrated that mutations within *COL7A1* are associated with the dystrophic forms of epidermolysis bullosa (DEB). DEB comprises a group of mechanobullous diseases characterized by cutaneous fragility with a tendency to form sub-basal lamina densa blisters (Christiano *et al.*, 1993; Pulkkinen and Uitto, 1999; Chen *et al.*, 2002a). In addition, targeted disruption of *COL7A1* in a mouse model demonstrated an almost identical phenotype to DEB in humans (Heinonen *et al.*, 1999). These results indicate that collagen VII is of critical importance for dermal–epidermal adhesion.

Approximately 300 distinct *COL7A1* mutations have been identified in DEB patients so far. Therapeutic introduction of *COL7A1* into skin cells is a promising treatment of DEB. Despite the relatively large size of *COL7A1*, the cDNA of which is still 9 kb makes gene transfer relatively problematic, and several methods including lentivirus- (Chen *et al.*, 2002b), retrovirus- (Baldeschi *et al.*, 2003) and ϕC31 integrase-based approaches (Ortiz-Urda *et al.*, 2002) have attempted to transfer *COL7A1* into keratinocytes. These studies used keratinocytes as target cells as collagen VII has been reported to be mainly synthesized and secreted by keratinocytes and to lesser extent by fibroblasts (Ryynanen *et al.*, 1992). However, application of gene-transferred DEB fibroblasts into the skin restored collagen VII expression in the dermal–epidermal junction (Ortiz-Urda *et al.*, 2003; Woodley *et al.*, 2003). In addition, using an intradermal injection of lentivirus with *COL7A1* induced the expression of collagen VII in fibroblasts and endothelial cells, resulting in collagen VII accumulation in the grafted DEB skin on the host animal (Woodley *et al.*, 2004).

[1]*Department of Dermatology, Hokkaido University Graduate School of Medicine, Sapporo, Japan*

Correspondence: Dr Daisuke Sawamura, Department of Dermatology, Hokkaido University Graduate School of Medicine, N15 W7, Sapporo 060-8638, Japan. E-mail: smartdai@med.hokudai.ac.jp

Abbreviations: DEB, dystrophic epidermolysis bullosa; FCS, fetal calf serum; VSV-G, G protein of vesicular stomatitis virus

Received 4 June 2005; revised 19 October 2005; accepted 3 November 2005; published online 26 January 2006

In this study, we have established a retroviral method to transfer *COL7A1* into DEB keratinocytes and fibroblasts. Next, we produced the skin grafts with gene-transferred keratinocytes or fibroblasts, and transplanted them into nude rats. Examination of collagen VII graft expression revealed that gene-transferred fibroblasts assembled more collagen VII in the form of anchoring fibrils beneath the basement membrane than gene-transferred keratinocytes. We conclude that fibroblasts are a more ideally suited target for *COL7A1* gene transfer than keratinocytes using retroviral gene therapy for the treatment of DEB.

RESULTS

Successful transfer COL7A1 using retroviral systems

We employed two retroviral vectors, pLIXN and pDON-AI, and full-length *COL7A1* cDNA was inserted into the retroviral vectors to generate plasmids termed pLI-COL and pDON-COL, respectively (Figure 1). Also, we created pDON(Δ) by removing the SV-40 promoter and *Neo* gene from pDON-AI and constructed a retroviral vector with *COL7A1* cDNA pDON(Δ)-COL (Figure 1). Several series of preliminary experiments demonstrated that retronectin (TAKARA) increased attachment of virus to keratinocytes and fibroblasts. Also, use of plasmid G protein of vesicular stomatitis virus (pVSV-G) (Pantropic System; Clontech, Palo Alto, CA) enabled concentration of viral particles by ultracentrifugation, resulting in an increase of transfer efficacy. After transfection of plasmids pLI-COL, pDON-COL, and pDON(Δ)-COL to 293 packaging cells, the culture media were collected. The virus titers (mean $\pm$ SD $\times$ 10^6/ml) of pLI-COL, pDON-COL, and pDON(Δ)-COL were $1.1 + 0.35$, $1.6 + 0.46$, and $2.7 + 0.55$, respectively.

We transferred *COL7A1* into cultured DEB keratinocytes and fibroblasts using the retroviral system. Transfection experiments showed that retroviral methods using pLI-COL and pDON-COL failed to introduce *COL7A1* to DEB cells (data not shown). Plasmid pDON(Δ)-COL with the VSV-G system allowed a greater gene transfer after further concentration of the virus particles increased the transfer rate (Figure 2). Immunostaining revealed that the transfer rates in DEB keratinocytes and fibroblasts were almost the same (Figures 2 and 3a), and immunoblotting demonstrated that the amount of collagen VII in their culture media was also identical (Figure 3b). The average copy number per cell of the *COL7A1* cDNA was evaluated by Southern blot analysis of genomic DNA extracted from the transduced cells. The result indicated that the intensities of 7.2 kb band from the integrated cDNA were the same in treated keratinocytes and fibroblasts, suggesting that integration copies for keratinocytes and fibroblasts was almost equal (Figure 3c). The copy number was estimated 2–3 by comparing with a serial dilution standard (data not shown).

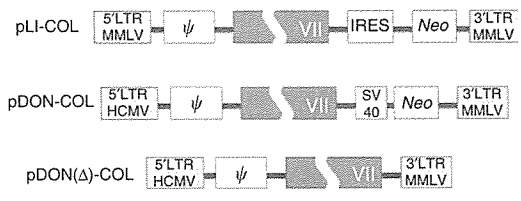

Figure 1. Schematic representation of retroviral *COL7A1* expression vectors. We employed two retroviral vectors, pLIXN (Clontech) and pDON-AI (Takara, Japan), and full-length *COL7A1* cDNA was inserted into the retroviral vectors to generate plasmids pLI-COL and pDON-COL, respectively. A pDON(Δ) vector was created by removing the SV-40 promoter and *Neo* gene from pDON-AI and *COL7A1* cDNA constructed retroviral vector made termed pDON(Δ)-COL. These vectors harbor long terminal repeat (LTR) derived from mouse moloney leukemia virus (MMLV) and human cytomegalovirus (HCMV). The internal ribosome entry site (IRES) enables expression of two unrelated reading frames from a single transcription unit. ψ: packaging signal.

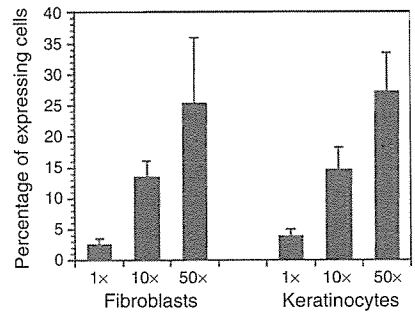

Figure 2. Successful gene transfer of *COL7A1* into DEB fibroblasts and keratinocytes using retroviral systems. *COL7A1* was transferred into DEB fibroblasts and keratinocytes using the retroviral systems. Immunostaining revealed that the transfer rates in DEB keratinocytes and fibroblasts were almost equal. The concentration of virus particles (by 10 or 50 times) using the VSV-G system improves the transfer rate. The values were represented the mean $\pm$ SD of six individual samples.

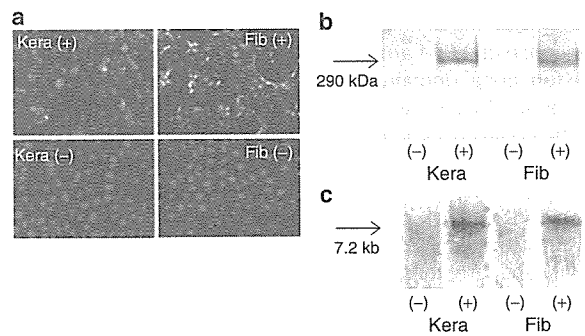

Figure 3. Corrective gene transfer of the *COL7A1* into DEB fibroblasts and keratinocytes. (**a**) Immnostaining showed that the gene-transfected DEB keratinocytes Kera (+) and fibroblasts Fib (+) expressed collagen VII, whereas no expression was found in either the untreated keratinocytes Kera (–) or fibroblasts Fib (–). Nuclei were counterstained with propidium iodide. (**b**) Western blot analysis demonstrated that the amount of transgene product in culture medium was almost the same between keratinocytes and fibroblasts. (**c**) Southern blot analysis of genomic DNA extracted from the transduced cells showed that the *COL7A1* cDNA integration copies for keratinocytes and fibroblasts were almost equal.

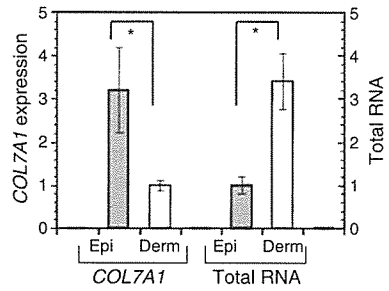

Figure 4. *In vivo COL7A1* expression in the epidermis is higher than that in the dermis. We measured *COL7A1* mRNA levels in the epidermis (Epi) and dermis (Derm) *in vivo*. Real-time PCR demonstrated that the *COL7A1*-specific signal (per RNA) of the epidermis was higher than that of the dermis. Comparison of the total RNA amounts from the epidermis and dermis in the same area of the excised normal skin showed that the amount from the dermis was higher than that from the epidermis. The *COL7A1* mRNA expression and total RNA amounts were expressed as an arbitrary scale. The values were represented the mean ± SD from three separate samples. $*P<0.01$, significant difference.

In vivo COL7A1 expression in epidermis is higher than that in dermis

To determine the *COL7A1* expression level in the epidermis and dermis *in vivo,* we separated the epidermis from the dermis, and measured *COL7A1* mRNA levels using real-time PCR. Real-time PCR demonstrated that the *COL7A1*-specific signal (per RNA) of the epidermis was higher than that of the dermis by 3.2-fold (Figure 4). Comparison of the total RNA amounts from the epidermis and dermis in the same area of the excised normal skin showed that the amount from the dermis was higher than that from the epidermis by 3.4-fold (Figure 4). Thus, the quantity of *COL7A1* expression in epidermis was significantly higher than that in dermis *in vivo*.

Gene-transferred fibroblasts can supply more collagen VII to the basement membrane zone than gene-transferred keratinocytes

We transplanted the gene-transferred DEB keratinocytes and fibroblasts into the wound of nude rats, and then observed *COL7A1* deposition 3, 6, and 9 weeks after transplantation. In the skin graft with gene-transferred keratinocytes and untreated fibroblasts, the *COL7A1* deposition was detectable in the basement membrane zone at 3 week and maintained this expression at least until 9 weeks (Figure 5). However, we found a greater accumulation of collagen VII in dermal–epidermal junction of the grafts using untreated keratinocytes and gene-transferred fibroblasts 3 weeks after transplantation. Furthermore, DEB fibroblasts transfected with *COL7A1* demonstrated more dermal–epidermal junction collagen VII staining than *COL7A1*-transfected DEB keratinocytes/untreated fibroblast (Figure 5) from 6 to 9 weeks. The grafts of DEB keratinocytes and fibroblasts as controls demonstrated no deposition (Figure 5). Semiquantification of *COL7A1* deposition in basement membrane zone in each point showed DEB fibroblasts with COL7A1 can supply higher amount of collagen VII to the basement membrane zone than DEB keratinocytes with *COL7A1* (Figure 6). Significant differences were found between the keratinocytes and fibroblasts samples at 3W and 9W points.

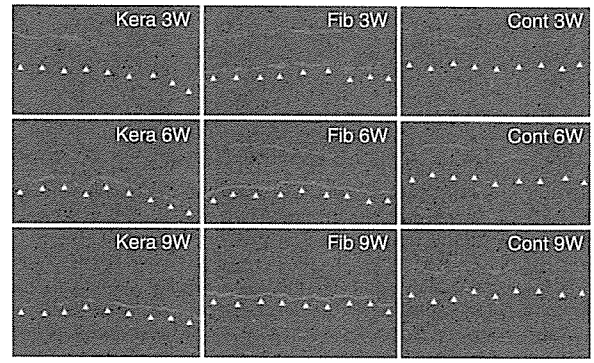

Figure 5. Gene-transferred fibroblasts can supply more collagen VII to the sub-basement membrane zone than gene-transferred keratinocytes. We transplanted gene-transferred DEB keratinocytes and DEB fibroblasts to nude rats wounded back skin, and observed *COL7A1* deposition by immunohistochemistry at 3, 6, and 9 weeks after transplantation. The skin graft with gene-transferred keratinocytes and untreated fibroblasts (Kera 3W, Kera 6W, Kera 9W) started dermal–epidermal junction collagen VII deposition at 3 week and maintained it until 9 weeks. A greater accumulation of collagen VII in dermal–epidermal junction of the grafts using untreated keratinocytes and gene-transferred fibroblasts was found 3 weeks after transplantation (Fib 3W). The DEB fibroblasts transfected with *COL7A1* demonstrated more dermal–epidermal junction collagen VII staining than *COL7A1*-transfected DEB keratinocytes/untreated fibroblast from 6 to 9 weeks (Fib 6W, Fib 9W). The control DEB keratinocyte and fibroblast cell grafts (Cont 3W, Cont 6W, Cont 9W) demonstrated no deposition. Arrowheads define the limit between the dermis and epidermis.

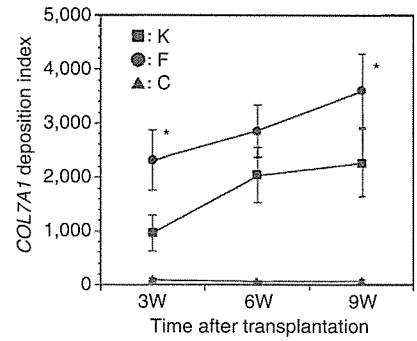

Figure 6. Semiquantification of *COL7A1* deposition in basement membrane zone. We transplanted gene-transferred DEB keratinocytes and DEB fibroblasts to nude rats wounded back skin, and observed *COL7A1* deposition by immunohistochemistry at 3, 6, and 9 weeks after transplantation. To semiquantify *COL7A1* deposition in basement membrane zone, we measured fluorescence intensity (arbitrary scale) in basement membrane zone at 10 areas at each point and the *COL7A1* deposition index was expressed as the mean ± SD from the 10 values. K: the skin graft with gene-transferred keratinocytes and untreated fibroblasts; F: the graft with untreated keratinocytes and gene-transferred fibroblasts grafts; C: the graft with untreated keratinocyte and untreated fibroblasts. $*P<0.01$, significant difference.

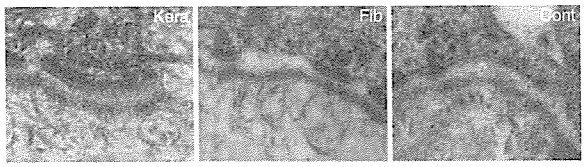

Figure 7. Collagen VII released from gene-transferred cells forms anchoring fibrils similar to normal skin. We examined the ultrastructural formation of anchoring fibrils in the grafts. The grafts with the gene-transferred keratinocytes (Kera) or the gene-transferred fibroblasts (Fib) demonstrated cross-banded, filamentous structures sometimes forming semicircular loops immediately beneath the lamina densa, corresponding to anchoring fibrils, whereas we failed to identify these filamentous structures in control without *COL7A1* transfection (Cont).

Collagen VII released from gene-transferred cells forms ultrastructurally normal anchoring fibrils

We examined the ultrastructural formation of anchoring fibrils in the graft. The grafts with both gene-transferred keratinocytes and fibroblasts demonstrated filamentous loop structures just beneath the lamina densa, which were corresponding to anchoring fibrils (Figure 7). We could not see any filamentous structures in control (untransfected) samples without *COL7A1*.

DISCUSSION

The developments in cloning the basement membrane protein genes have allowed the identification of the causative genes/proteins harboring the mutations responsible for this group of epidermolysis bullosa diseases (Uitto and Pulkkinen, 2001). We can now make good estimations about the prognosis and severity of these diseases with profound beneficial effects on genetic counseling and DNA-based prenatal diagnosis. However, patients most frequently desire an appropriate therapy for epidermolysis bullosa. Corrective transfer of the *COL7A1* gene back into the skin cells is a promising treatment of DEB.

The previous Northern hybridization study revealed a high level of *COL7A1* mRNA expression in cultured epidermal keratinocytes, whereas the expression was lower in cultured dermal fibroblasts (Ryynanen *et al.*, 1992). These results indicate that epidermal keratinocytes and dermal fibroblasts express the collagen VII, but also suggest that epidermal keratinocytes are the primary source of collagen VII in developing human skin. Many investigators have utilized keratinocytes as the target cells of DEB gene therapy. Several methods including viral- (Ghazizadeh and Taichman, 2000) and non-viral-mediated transduction (Vogel, 2000) have been reported for *in vivo* and *ex vivo* gene transfer into keratinocytes. *COL7A1* cDNA was recently transferred into cultured DEB keratinocytes using some methods including lentivirus- (Chen *et al.*, 2002b), retrovirus- (Baldeschi *et al.*, 2003) and ϕC31 integrase-based approaches (Ortiz-Urda *et al.*, 2002). The corrected DEB keratinocytes expressed the recombinant collagen VII and restored the *in vivo* synthesis of anchoring fibrils after implantation, demonstrating the feasibility of gene transfer using DEB keratinocytes. We also succeeded in transferring the *COL7A1* into *in vivo* keratinocytes using the naked DNA method (Sawamura *et al.*, 2002) although the *COL7A1* transfer efficacy was lower than the above *ex vivo* method.

Many gene therapy protocols have already utilized retroviral vectors for clinical practices. In this study, we also showed a retroviral vector could transfer the 9 kb *COL7A1* cDNA into DEB keratinocytes. Another group has succeeded in transducing *COL7A1* gene to keratinocytes using a retroviral plasmid containing the Neo selection gene (Baldeschi *et al.*, 2003). They showed that transduction efficacies to primary keratinocytes were 40 and 83–93% by retroviral vectors pLSRS-Ires-zero and pMSCV, respectively. However, the use of similar plasmids is not possible to efficiently introduce this gene into keratinocytes in our experiments. In our system, the efficacy was about 30%, which was lower than those in previous report. This study, as far as we know, has been the first to try a retronectin retroviral targeting system for keratinocytes. Retronectin is a recombinant peptide, which consists of three functional fibronectin domains and significantly enhances retrovirus-mediated gene transduction into mammalian cells. Our data showed that addition of retronectin increased transfer efficacy in keratinocytes by 3-fold (data not shown), indicating that retronectin is indeed efficient in this keratinocyte/retroviral system.

Some groups have succeeded in transferring this gene into keratinocytes as mentioned above. On the other hand, cutaneous injection of the DEB fibroblasts transduced using ϕC31 integrase-based approach also restores collagen VII deposition along the dermal–epidermal junction (Ortiz-Urda *et al.*, 2003). Also, gene-corrected DEB fibroblasts and normal human fibroblasts alone could supply type VII collagen deposition at the basement membrane zone *in vivo* (Woodley *et al.* 2003), and this implies a possibility that normal cultured human dermal fibroblasts are injected intradermally into recesive dystrophic epidermolysis bullosa patients' skin. Moreover, intradermal injection of lentiviral vector with *COL7A1* increased collagen VII expression in fibroblasts and endothelial cells, resulting in stronger deposition of collagen VII along the basement membrane zone anchoring fibrils as seen by electron microscopy (Woodley *et al.*, 2004). This study also introduced the *COL7A1* gene into DEB fibroblasts using the retroviral method and the consequent collagen VII assembly beneath the basement membrane of the fibroblast containing graft.

In this study, we compared dermal fibroblasts and epidermal keratinocytes as efficient target recipient cells for the collagen VII transgene product. After retroviral introduction of *COL7A1*, the transfer efficacy and the amount of collagen VII in the cultured keratinocytes media supernatant are almost the same as those of fibroblasts. Interestingly, a series of skin graft experiments first demonstrated that gene-transfected fibroblasts more efficiently assembled collagen VII into the dermal–epidermal junction than the gene-transferred keratinocytes. Previous Northern blotting analysis revealed higher level of *COL7A1* mRNA expression in cultured epidermal keratinocytes than fibroblasts (Ryynanen

et al., 1992). This study utilized real-time PCR technique and confirmed that the epidermis produced much more collagen VII than the dermis *in vivo*. If gene-transferred fibroblasts and keratinocytes express similar amounts of type VII collagen also *in vivo*, the fibroblasts may have a better ability to supply type VII collagen to the basement membrane than the keratinocytes.

It is evident that expression of recombinant collagen VII is driven by heterologous promoters, which escape the regulatory mechanisms that govern the expression of endogenous collagen VII in the different cell types. Also, keratinocytes have been preferred because of the possibility they offer of targeting stem cells and compared to keratinocytes, fibroblasts rapidly senesce *in vivo* (Krueger, 2000). However, fibroblasts are more robust and less susceptible to growth arrest and differentiation than epidermal keratinocytes (Ortiz-Urda *et al.*, 2003). Furthermore, genetically engineered fibroblasts have had their use explored for therapeutic applications including visceral and cutaneous implantation to supply gene products to circulation (Roth *et al.*, 2001). Given the above combined factors, it is proposed that fibroblasts may be potentially more feasible and a better target of DEB gene therapy than keratinocytes.

MATERIALS AND METHODS

Cell culture

Primary keratinocytes were isolated and grown in the presence of an irradiated 3T3 feeder layer (Rheinwald and Green, 1975). Briefly, keratinocytes, which were obtained from skin biopsy of a DEB patient and healthy controls, were cultured on feeder layers of mitomycin C-treated mouse 3T3 fibroblasts in DMEM: Ham's F-12 (3:1) supplemented with 10% fetal calf serum (FCS), 5 μg/ml insulin, 10 ng/ml epidermal growth factor, 0.4 μg/ml hydrocortisone, and 8 ng/ml cholera toxin. The DEB patient was diagnosed as the most severe subtype, and Hallopeau–Siemens type showed no *COL7A1* expression in the skin and harbored heterozygous premature stop codon mutations 1474del8 and 5818delC. Fibroblasts were also obtained from skin biopsy from the DEB patient and healthy controls, and were cultured in DMEM with 10% FCS. Packaging cells amphopack-293 and GP2-293 (Clontech, Palo Alto, CA) were maintained in DMEM with 10% FCS, 2 mM glutamine, and 2 mM sodium pyruvate.

Informed consents were obtained from all individual subjects in this study. The protocols were approved by the Ethical Committee at Hokkaido University Graduate School of Medicine. This study was conducted according to the Declaration of Helsinki Principles.

Intrinsic expression of collagen VII in control keratinocytes and fibroblasts

Human skin was obtained from normal volunteers, and treated with 10 mg/ml dispase for 3 hours at 37°C to separate the epidermis from the dermis. The epidermal and dermal sheets were minced and total RNA was extracted using an RNeasy RNA extraction kit (Qiagen, Hilden, Germany). First-strand cDNA was synthesized with reverse transcriptase (Life Sciences Inc., St Petersburg, FL) using an oligo-dT primer. Assays-on-Demand™ Products for *COL7A1* and *GAPDH* were purchased from Applied Biosystems (Foster City, CA). The 50 μl reaction in each well contained 1 μl of total cDNA, 300 nM sequence-specific primers, and 200 nM dual-labeled fluorogenic probe with 1 U of Taqman Universal PCR master mix (Applied Biosystems). A negative control PCR without template and a positive PCR control with a template of known amplification were included in each assay. The samples underwent the following stages: stage 1, 50°C for 2 minutes; stage 2, 95°C for 10 minutes; and stage 3, 95°C for 15 seconds, followed by 60°C for 1 minutes. Stage 3 was repeated 45 times. Gene-specific products were measured by means of an ABI Prism 7700 sequence detection system (Perkin-Elmer Applied Biosystems, Foster City, CA) continuously for 45 cycles. The *COL7A1*-specific signal was normalized by constitutively expressed *GAPDH* and expressed as arbitrary scale.

Construction of retroviral COL7A1 expression vectors and transfection

Human full-length *COL7A1* cDNA was constructed from several overlapping cDNA clones (Sawamura *et al.*, 2002). We employed two retroviral vectors, pLIXN (Clontech) and pDON-AI (Takara, Otsu, Japan), and full-length *COL7A1* cDNA was inserted into the retroviral vectors to generate plasmids termed pLI-COL and pDON-COL, respectively (Figure 1). Also, we created pDON(Δ) by removing the SV-40 promoter and *Neo* gene from pDON-AI and constructed a retroviral vector with *COL7A1* cDNA pDON(Δ)-COL (Figure 1). The recombinant retroviruses were produced by transfecting the retroviral plasmids into the amphotropic amphopack-293 packaging cells (Clontech) using calcium-phosphate coprecipitation. In addition, we tried VSV-G-pseudotyped retrovirus vectors. The retroviral plasmids and plasmid pVSV-G were cotransfected into pantropic GP2-293 packaging cells (Clontech). The viral particles were recovered from the cell culture medium 48 hours later and applied to keratinocyte or fibroblast cultures. To increase transfer efficacy, ultracentrifugation was performed to concentrate the VSV-G virus particles. The titer of the viral supernatant was determined by real-time quantitative PCR (Towers *et al.*, 1999).

Cells infection with retrovirus

Keratinocytes and fibroblasts were cultured to up to 60% of confluency and then infected with the viral suspensions in 5 μg/ml polybrene. To increase the virus–cell interactions, we coated the surface of the culture plates with 10 ng/ml retronectin (Takara; fibronectin fragment CH-296). After incubation for 24 hours at 32°C, we maintained the treated cells under fresh medium for another 24 hours until the transduction efficiency was assessed by immunofluorescence examination of the infected cells.

Immunostaining and immunoblot

Transfected cultured keratinocytes and fibroblasts were fixed with 2% parafromaldehye in phosphate-buffered saline, and were then incubated with the monoclonal antibody LH7.2 (1:100) against the NC1 domain of collagen VII (Chemicon, Temecula, CA) for 18 hours at 4°C. They were treated with secondary goat anti-mouse IgG antibodies conjugated with FITC (1:50) for 1 hour at 37°C, and preparations were examined under a fluorescence microscope. Nuclei were counterstained with propidium iodide (Dojindo Laboratories, Kumamoto, Japan). Subconfluent cell cultures were fed for 48 hours with serum-free medium supplemented with 50 μg/ml ascorbic acid. For SDS-PAGE analysis, the culture medium was

treated with Amicon Ultra-100,000 Centrifugal Filter Devices (Millipore, Bedford, MA) for concentration and desalting. The samples were separated on a 5% polyacrylamide gel under reducing conditions. Immunoblotting analysis was performed by treating with the LH7.2 monoclonal antibody (1:1,000) for 18 hours at 4°C, and then secondary goat anti-mouse IgG antibodies conjugated with peroxidase (1:2,000) for 1 hour at 37°C. The resultant complexes were processed for Phototope HRP Western Blot Detection System (Cell Signaling, Beverly, MA) according to the manufacturer's protocol.

Southern blot analysis

The average copy number per cell of the *COL7A1* cDNA was evaluated by Southern blot analysis (Baldeschi *et al.*, 2003). Briefly, genomic DNA was extracted from subconfluent cell cultures and digested with *Bgl*II and *Hind*III. Plasmid pDON(Δ)-COL was serially diluted with yeast genomic DNA at the final concentration ranging from 0.5 to 20 copies/cell. The digested DNA was electrophoresed on a 0.8% agarose gel and transferred to Zeta-Probe membrane (Bio-Rad, Hercules, CA). The 375 bp cDNA extending from exons 58 to 64 was generated by PCR amplification of *COL7A1* cDNA as a template. This fragment was designed to recognize a 7.2 kb band from the integrated cDNA, and also 1.0 and 0.3 kb bands from the intrinsic *COL7A1* gene. The membranes were hybridized with the 375 bp cDNA probe was labeled by random primed incorporation of digoxigenin-labeled 2′-deoxyuridine 5′-triphosphate using the DIG DNA Labeling Kit (Roche, Indianapolis, IN) according to the manufacturer's instructions. After high stringency washes, blots were visualized using an enhanced chemiluminescence system.

Grafting of gene-transferred DEB cells

Gene-transferred and untreated DEB keratinocytes and DEB fibroblasts were cultured using the above methods. Fibroblasts (10^6) were seeded into a collagen sponge scaffold and maintained in DMEM with 10% FCS for 3 days. In nude rats (F344/N Jcl-rnu), the sites for transplantation were prepared by excising a 2 cm^2 area of dorsal epidermis and dermis, and then the collagen sponge (3 cm^2) containing the fibroblasts was placed into the skin wound. The confluent cultures of 10^6 keratinocytes were treated with dispase (1 nU/ml; Godo Shusei, Tokyo, Japan), and the floating epidermal sheet placed on the collagen sponge. Preliminary experiment showed that the number of fibroblasts was almost equal to that of keratinocytes when we applied the graft to the animal. An occlusive dressing was quickly placed over the graft to hold it in position and to prevent it from drying out and then the dressing was removed after 7 days. We prepared combinations of gene-transferred keratinocytes and untreated fibroblasts, of untreated keratinocytes and gene-transferred fibroblasts, and of untreated keratinocytes and fibroblasts as control. Skin biopsies were taken from the grafted skin at various time points and subjected to routine immunohistochemical staining using the LH7.2 monoclonal antibody and ultrastructural analysis. To semiquantify *COL7A1* accumulation in basement membrane zone, we converted color images to gray-scale images, and measured fluorescence intensity (arbitrary scale) in basement membrane zone at 10 areas using NIH Image software. The *COL7A1* deposition index was expressed as the mean ± SD from the 10 values.

CONFLICT OF INTEREST
The authors state no conflict of interest.

ACKNOWLEDGMENTS
We wish to thank Dr James R McMillan for proof reading and comments concerning this manuscript. This work was supported in part by Grants-in-Aid from the Ministry of Education, Science, Sports, and Culture of Japan to D Sawamura (15390337, 17659331) and H Shimizu (15390336, 17209038), and by grants from the Ministry of Health of Japan to H Shimizu (H13-Specific Disease-02, H16-Intractable Disease-05).

REFERENCES

Baldeschi C, Gache Y, Rattenholl A, Bouille P, Danos O, Ortonne JP *et al.* (2003) Genetic correction of canine dystrophic epidermolysis bullosa mediated by retroviral vectors. *Hum Mol Genet* 12:1897–905

Burgeson RE (1993) Type VII collagen, anchoring fibrils, and epidermolysis bullosa. *J Invest Dermatol* 101:252–5

Chen M, Costa FK, Lindvay CR, Han YP, Woodley DT (2002a) The recombinant expression of full-length type VII collagen and characterization of molecular mechanisms underlying dystrophic epidermolysis bullosa. *J Biol Chem* 277:2118–24

Chen M, Kasahara N, Keene DR, Chan L, Hoeffler WK, Finlay D *et al.* (2002b) Restoration of type VII collagen expression and function in dystrophic epidermolysis bullosa. *Nat Genet* 32:670–5

Christiano AM, Greenspan DS, Hoffman GG, Zhang X, Tamai Y, Lin AN *et al.* (1993) A missense mutation in type VII collagen in two affected siblings with recessive dystrophic epidermolysis bullosa. *Nat Genet* 4:62–6

Christiano AM, Greenspan DS, Lee S, Uitto J (1994a) Cloning of human type VII collagen, complete primary sequence of the alpha 1(VII) chain and identification of intragenic polymorphisms. *J Biol Chem* 269:20256–62

Christiano AM, Hoffman GG, Chung-Honet LC, Lee S, Cheng W, Uitto J *et al.* (1994b) Structural organization of the human type VII collagen gene (COL7A1), composed of more exons than any previously characterized gene. *Genomics* 21:169–79

Ghazizadeh S, Taichman LB (2000) Virus-mediated gene transfer for cutaneous gene therapy. *Hum Gene Ther* 11:2247–51

Heinonen S, Mannikko M, Klement JF, Whitaker-Menezes D, Murphy GF, Uitto J (1999) Targeted inactivation of the type VII collagen gene (Col7a1) in mice results in severe blistering phenotype: a model for recessive dystrophic epidermolysis bullosa. *J Cell Sci* 112:3641–8

Krueger GG (2000) Fibroblasts and dermal gene therapy. *Hum Gene Ther* 11:2289–96

Ortiz-Urda S, Lin Q, Green CL, Keene DR, Marinkovich MP, Khavari PA (2003) Injection of genetically engineered fibroblasts corrects regenerated human epidermolysis bullosa skin tissue. *J Clin Invest* 111:251–5

Ortiz-Urda S, Thyagarajan B, Keene DR, Lin Q, Fang M, Calos MP *et al.* (2002) Stable nonviral genetic correction of inherited human skin disease. *Nat Med* 8:1166–70

Pulkkinen L, Uitto J (1999) Mutation analysis and molecular genetics of epidermolysis bullosa. *Matrix Biol* 18:29–42

Rheinwald JG, Green H (1975) Serial cultivation of strains of human epidermal keratinocytes: the formation of keratinizing colonies from single cells. *Cell* 6:331–43

Roth DA, Tawa NE Jr, O'Brien JM, Treco DA, Selden RF (2001) Factor VIII Transkaryotic Therapy Study Group: nonviral transfer of the gene encoding coagulation factor VIII in patients with severe hemophilia A. *N Engl J Med* 344:1735–42

Ryynanen J, Sollberg S, Parente MG, Chung LC, Christiano AM, Uitto J (1992) Type VII collagen gene expression by cultured human cells and in fetal skin, abundant mRNA and protein levels in epidermal keratinocytes. *J Clin Invest* 89:163–8

Sawamura D, Yasukawa K, Kodama K, Yokota K, Sato-Matsumura KC, Toshihiro T *et al.* (2002) The majority of keratinocytes incorporate intradermally injected plasmid DNA regardless of size but only a small proportion of cells can express the gene product. *J Invest Dermatol* 118:967–71

Towers GJ, Stockholm D, Labrousse-Najburg V, Carlier F, Danos O, Pages JC (1999) One step screening of retroviral producer clones by real time quantitative PCR. *J Gene Med* 1:352–9

Uitto J, Chung-Honet LC, Christiano AM (1992) Molecular biology and pathology of type VII collagen. *Exp Dermatol* 1:2–11

Uitto J, Pulkkinen L (2001) Molecular genetics of heritable blistering disorders. *Arch Dermatol* 137:1458–61

Vogel JC (2000) Nonviral skin gene therapy. *Hum Gene Ther* 11:2253–9

Woodley DT, Keene DR, Atha T, Huang Y, Ram R, Kasahara N *et al.* (2004) Intradermal injection of lentiviral vectors corrects regenerated human dystrophic epidermolysis bullosa skin tissue *in vivo*. *Mol Ther* 10: 318–326

Woodley DT, Krueger GG, Jorgensen CM, Fairley JA, Atha T, Huang Y *et al.* (2003) Normal and gene-corrected dystrophic epidermolysis bullosa fibroblasts alone can produce type VII collagen at the basement membrane zone. *J Invest Dermatol* 121:1523–747

ORIGINAL ARTICLE

Targeted Skipping of a Single Exon Harboring a Premature Termination Codon Mutation: Implications and Potential for Gene Correction Therapy for Selective Dystrophic Epidermolysis Bullosa Patients

Maki Goto[1], Daisuke Sawamura[1], Wataru Nishie[1], Kaori Sakai[1], James R. McMillan[1], Masashi Akiyama[1] and Hiroshi Shimizu[1]

This study examined the feasibility of antisense oligoribonucleotide (AON) therapy for dystrophic epidermolysis bullosa (DEB). AON was designed to induce skipping of a targeted exon containing a premature termination codon mutation, resulting in restoration of the open reading frame. We targeted exon 70 of *COL7A1*, as a recurrent mutation 5818delC in Japanese DEB patients was localized to exon 70. We found that one AON induced effective skipping of normal exon 70 containing 16 amino acids. Attachment and migration analyses showed that recombinant collagen without contribution of exon 70 was similar in effect to normal type VII collagen. Next, we synthesized mutation-specific AON by deleting cytosine at 5818. Introduction of this AON into DEB keratinocytes harboring 5818delC showed that the AON induced skipping of exon 70 in the abnormal 5818delC allele. Furthermore, 6.2% of DEB keratinocytes started to express type VII collagen *in vitro* after application of the mutation-specific AON. Injection of the AON into rat model grafted with DEB keratinocytes and fibroblasts induced a low amount of type VII collagen expression. We conclude that skipping of targeted exons using mutation-specific AON may show potential for future gene therapy for DEB patients.

Journal of Investigative Dermatology (2006) **126,** 2614–2620. doi:10.1038/sj.jid.5700435; published online 15 June 2006

INTRODUCTION

The transfer of normal genes into somatic cells is one strategy to treat patients with genetic diseases. However, this strategy still encounters problems including efficacy of gene transfer rate and practical clinical safety. Thus, other strategies, including pharmacological therapy or gene correction, are receiving increasing attention.

Recently, studies of muscular dystrophy have demonstrated the feasibility of modulating intron-exon splicing using antisense oligoribonucleotides (AONs), which may induce exon skipping, resulting in slightly shorter, but in-frame, mRNA transcripts (Mann *et al.*, 2001; Lu *et al.*, 2003). In muscular dystrophy caused by mutations in the dystrophin gene, shorter transcripts found in patients with milder phenotypes have a significantly longer life expectancy when compared to the patients with a complete loss of dystrophin expression (Monaco *et al.*, 1988; England *et al.*, 1990). These observations have led to the idea of using AON to skip abnormal, mutated exons to restore the open reading frame and convert a severe phenotype into a milder form (Mann *et al.*, 2001; Lu *et al.*, 2003). The mechanism of exon skipping is based upon AON, small synthetic RNA molecules that are designed to bind to specific sequences within the pre-mRNA (Mayeda *et al.*, 1990; Galderisi *et al.*, 1999).

Dystrophic epidermolysis bullosa (DEB) is clinically characterized by mucocutaneous blistering in response to minor trauma, followed by scarring and nail dystrophy, and patients generally exhibit tissue separation beneath the lamina densa of the epidermal basement membrane where anchoring fibrils are present in normal skin but structurally compromised in DEB (Fine *et al.*, 2000). DEB is caused by mutations in the *COL7A1* gene encoding type VII collagen, the major component of anchoring fibrils (Uitto *et al.*, 1995; Fine *et al.*, 2000). Several methods have achieved transfer of normal *COL7A1* into the patients' skin (Chen *et al.*, 2002; Ortiz-Urda *et al.*, 2002; Goto *et al.*, 2006), but this has never yet been extended to patients in clinical practice.

Previous report demonstrated an interesting DEB case whose manifestation was milder than expected from mutations in genomic DNA (McGrath *et al.*, 1999). Further mRNA analysis revealed that the mutation led to skipping of that single exon and subsequent maintenance of the open reading

[1]*Department of Dermatology, Hokkaido University Graduate School of Medicine, Sapporo, Japan*

Correspondence: Dr Daisuke Sawamura, Department of Dermatology, Hokkaido University Graduate School of Medicine, N15 W7, Sapporo 060-8638, Japan. E-mail: smartdai@med.hokudai.ac.jp

Abbreviations: AON, antisense oligoribonucleotide; DEB, dystrophic epidermolysis bullosa; HS-RDEB, Hallopeau–Siemens recessive DEB; RT-PCR, reverse transcriptase-PCR

Received 2 February 2006; revised 20 March 2006; accepted 4 April 2006; published online 15 June 2006

frame. In addition, missense mutations are known to provide unexpected *COL7A1* splicing outcomes (Wessagowit *et al.*, 2005). The *COL7A1* mutations causing single exon skipping resulted in milder cases than the predicted Hallopeau–Siemens recessive DEB phenotype (HS-RDEB) with nonsense mutations (Terracina *et al.*, 1998).

In this study, we have examined the feasibility of using AON in targeted exon skipping to modulate *COL7A1* splicing in such a manner that the translational open reading frame can be restored in keratinocytes from DEB patients.

RESULTS

Detection of exon 70 skipping in cultured keratinocytes

We targeted exon 70 for AON therapy as the recurrent premature termination codon mutation 5818delC in DEB patients was localized to exon 70 (Tamai *et al.*, 1999; Sawamura *et al.*, 2005). We synthesized two potential AONs, h70AON1 and h70AON2, which comprised full-length phosphorothioate backbone and HPLC-purified 2′-*O*-methyl-modified ribose molecules (Figure 1a). To evaluate the effects of h70AON1 and h70AON2 on *COL7A1* skipping of normal exon 70, we introduced them to HaCaT keratinocytes or normal human epidermal keratinocytes, and amplified *COL7A1* cDNA by reverse transcriptase-PCR (RT-PCR) with the forward primer on the border of exons 65 and 66, and a reverse primer on exon 72 (66–72 primer set). The h70AON1 samples showed a single 347 bp band. In the h70AON2 experiment, the samples showed a strong upper 347 bp band, whereas the lower 299 bp band was apparent (Figure 1b). Sequence analysis revealed that the upper 347 bp band consisted of exons 66, 67, 68, 69, 70, 71, and 72, whereas a lack of exon 70 was found in the lower 299 bp band. To semiquantify the amount of the lower and upper bands, we subcloned the PCR product to the TA cloning vector. The rate of the lower band to the upper band was expressed as the exon skipping rate. The result showed that the rates in samples of HaCaT cells and normal human keratinocytes were 18.2 and 28.1%, respectively. Each value represents the mean ± SD of four samples.

These results indicate that h70AON2 could induce skipping of exon 70. We simultaneously performed a time-course experiment, in which *COL7A1* expression in cultured HaCaT cells was examined 8, 16, 24, 48, and 72 hours after h70AON2 transfer. We found the highest expression of the 299 bp band at 16hours after AON transfer, although the effect of AON was totally extinct 72 hours after the transfer (Figure 1c). We obtained the samples 16 hours after transfer of h70AON2 for further experiments.

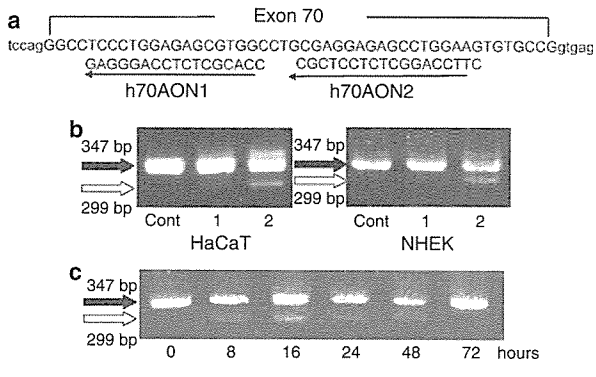

Figure 1. Detection of exon 70 skipping in cultured keratinocytes. The recurrent premature termination codon mutation 5818delC in DEB patients was localized to exon 70. We introduced h70AON1 and h70AON2 into HaCaT keratinocytes or normal human keratinocytes (NHEK), and amplified *COL7A1* cDNA by RT-PCR with the 66–72 primer set. (**a**) Sequences of h70AON1 and 2 are shown. (**b**) The h70AON1 samples (1) showed a single 347 bp band containing exon 70 (black arrow). The h70AON2 samples (2) showed an upper strong 347 bp band with exon 70 (black arrow), whereas the weaker lower 299 bp band without exon 70 (white arrow) was apparent. Only the 347 bp band was found in control samples without AON treatment (Cont). (**c**) We performed a time-course experiment, in which *COL7A1* expression in cultured HaCaT cells was examined 8, 16, 24, 48, and 72 hours after h70AON2 transfer. We found the highest expression of the 299 bp band at the 16 hours after AON transfer although the effect of AON was totally extinct 72 hours after the transfer.

Detection of exon 70 skipping *in vivo*

To simulate AON therapy in clinical practice, we transplanted human skin onto a nude rat and then injected 30 μg of h70AON2 to the graft. Saline was injected in a control. After 16 hours, the skin biopsies were taken from the injected site and were subjected to RT-PCR analysis. RT-PCR with the 66–72 primer set amplified a 347 bp strong band containing exon 70 and a weak signal of 299 bp band without exon 70 from the treated sample, whereas the control sample showed 347 bp band alone (Figure 2). We also applied 0.3 or 3 μg of h70AON2 to the graft, resulting in no signal of 299 bp band (data not shown). TA cloning of the 30 μg h70AON2 samples showed that the proportion of the lower band to the upper bands was 12.2%. To verify exon 70 skipping, we synthesized a 70Δ primer set with a forward primer on border of exons 63 and 64, and reversel primer on the border of exons 69 and 71. RT-PCR amplification with the 70Δ primer set detected a 305 bp band in only the AON-treated samples, which were indicative of exon skipping of 70 (Figure 2).

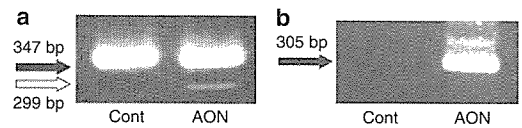

Figure 2. Detection of exon 70 skipping *in vivo*. We transplanted human skin to a nude rat and then injected 30 μg of h70AON2 AON into the graft. After 16 hours, the skin biopsies were taken from the injected site and were subjected to RT-PCR analysis. (**a**) RT-PCR with the 66–72 primer set amplified a 347 bp strong band (black arrow) containing exon 70 and a weaker signal of 299 bp band (white arrow) without exon 70 from the (AON)-treated sample, whereas the control sample showed a 347 bp band alone (Cont). (**b**) RT-PCR amplification with the 70Δ primer set detected a 305 bp band only in AON-treated samples. The AON lane seemed to have the higher molecular weight band in addition to the 305 bp *COL7A1* band. However, subcloning of PCR product to a TA cloning vector (Invitrogen, Carlsbad, CA) could not detect the corresponding *COL7A1* cDNA and we thought it to be a PCR artifact.

Assays for type VII collagen without exon 70

There is a possibility that the deletion of 16 amino acids, which are encoded by exon 70, may abolish some of the functions of type VII collagen. Therefore, we prepared retrovirus vector containing *COL7A1* cDNA without exon 70, and introduced the gene to keratinocytes from HS-RDEB patient who harbored heterozygous *COL7A1* 5818delC and 1474del8 mutations, and showed no expression of type VII collagen in immunofluorescence level as mentioned below (Goto *et al.*, 2006). The Western blot of the supernatant showed that HS-RDEB keratinocytes began to express type VII collagen after gene introduction (Figure 3a). The amounts of secreted collagen were almost identical in culture media between the normal *COL7A1* and *COL7A1*Δ70 samples. Subsequently, the cultured keratinocytes supernatant and the keratinocytes themselves were used for *in vitro* and *in vivo* studies. Cell migration assay using normal keratinocytes showed that the supernatants both with *COL7A1* and *COL7A1*Δ70 samples had a similar effect on the migration of normal keratinocytes (Figure 3b). The cell adhesion assay also demonstrated that *COL7A1*Δ70 supernatant had almost the same adhesive properties for the cells as normal *COL7A1* (Figure 3c). Furthermore, we constructed artificial skin grafts using untreated HS-RDEB fibroblasts and HS-RDEB keratinocytes transduced with *COL7A1* and *COL7A1*Δ70, and then applied them to a nude rat model. Ultrastructural analysis of the grafts showed formation of anchoring fibrils in both samples with *COL7A1* and *COL7A1*Δ70 samples (Figure 4). These results demonstrated that type VII collagen that lacks 16 amino acids of exon 70 might have similar properties to normal type VII collagen, suggesting that exon 70 skipping by AON is promising.

Elucidation of AON specific for 5818delC mutation

We designed mutation-specific AON hm70AON by deleting cytosine at 5818 (Figure 5a). Then we introduced hm70AON to normal human keratinocytes and HS-RDEB keratinocytes and performed the following RT-PCR analysis. The sample from HS-RDEB keratinocytes showed two PCR bands with or without exon 70, whereas a strong upper single band was observed in of the sample from normal human keratinocytes (Figure 5b). This indicated that the hm70AON induced skipping of exon 70 predominantly in abnormal allele with the 5818delC mutation. The sample from HS-RDEB keratinocytes without the AON treatment as control also showed the single band. TA cloning of the PCR samples showed that the exon skipping rates of HS-RDEB and normal keratinocyte samples were 18.5 and 1.3%, respectively; therefore, hm70AON induced skipping of exon 70 predominantly in abnormal allele with 5818delC. This HS-RDEB patient harbored heterozygous *COL7A1* 5818delC and 1474del8 mutations, and RT-PCR analysis using the keratinocyte cDNA showed no naturally occurring skipping of exon 70 containing the frameshift mutation (Figure 5b). Immunofluorescence analysis demonstrated using type VII collagen no expression of type VII collagen (Figure 5c) and ultrastructural study

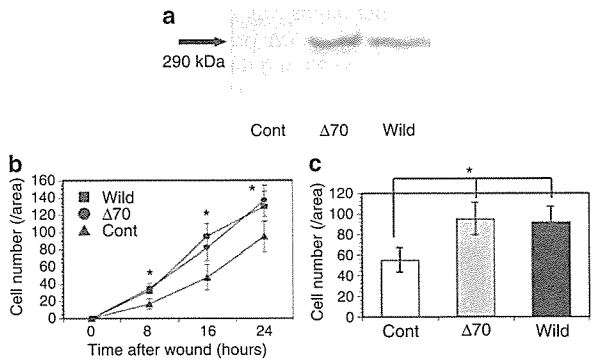

Figure 3. Assays for the type VII collagen without exon 70. We prepared retrovirus vectors with normal *COL7A1* cDNA (Wild) or *COL7A1* cDNA without exon 70 (Δ70), and introduced the gene into DEB keratinocytes, which showed no expression of any type VII collagen. (**a**) The Western blot of the supernatant showed that the amount of secreted type VII collagen in the culture media was almost similar to that of the normal *COL7A1* and *COL7A1*Δ70 samples. Cont: no transfection. (**b**) Cell migration assay showed that the supernatants from both *COL7A1* and *COL7A1*Δ70 samples had a similar effect on normal human keratinocyte migration. (**c**) The cell adhesion assay also demonstrated that *COL7A1*Δ70 supernatant had almost the same adhesive ability for normal keratinocytes as that of *COL7A1* (Figure 3). Each value represents mean±SD of six samples. *$P<0.01$: significant difference between cont *versus* wild or cont *versus* Δ70 samples.

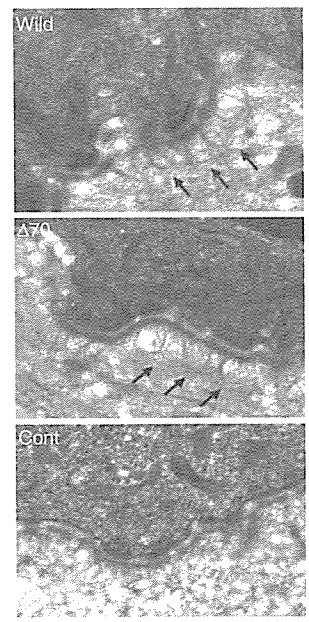

Figure 4. Formation of anchoring fibrils containing COL7A1Δ70. We constructed artificial skin grafts using DEB fibroblasts and keratinocytes transduced with wild-type *COL7A1* or *COL7A1*Δ70, and then grafted them onto a nude rat model. Ultrastructural analysis of the grafts showed that formation of anchoring fibrils could be identified in both samples with *COL7A1*- and *COL7A1*Δ70-transfected cells. Although no obvious anchoring fibrils were observed in control grafts with untransfected DEB keratinocytes alone (Cont), there were wisp-like structures below the lamina densa.

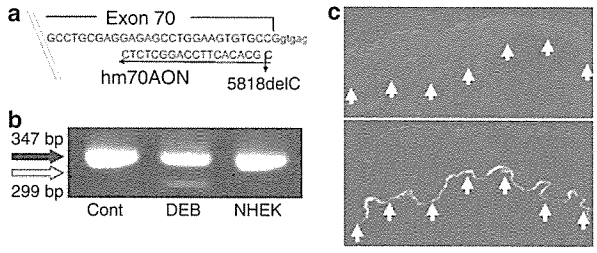

Figure 5. **Elucidation of AONs specific for 5818delC mutation.** We introduced mutation-specific AON hm70AON into normal human keratinocytes and DEB keratinocytes and performed the following RT-PCR analysis. (**a**) Sequences of mutation-specific AON hm70AON are shown. (**b**) The sample from DEB keratinocytes showed two PCR bands with exon 70 (347 bp) or without exon 70 (299 bp), whereas there was little or no lower band (299 bp) observed in the normal human keratinocytes sample (NHEK). Cont: the sample from DEB keratinocytes without the AON treatment. This HS-RDEB patient harbored heterozygous *COL7A1* 5818delC and 1474del8 mutations and RT-PCR analysis showed no naturally occurring skipping of exon 70 containing the frameshift mutation. (**c**) Immunofluorescence analysis of the patient using type VII collagen antibody demonstrated no expression of type VII collagen (the upper panel). The lower panel shows the expression from normal control. Arrows indicate epidermal-dermal junction.

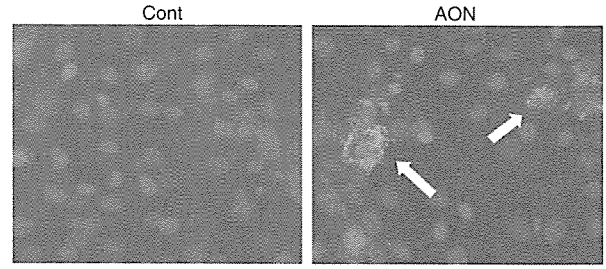

Figure 6. **Rescue of type VII collagen expression in DEB keratinocytes *in vitro*.** We transfected the hm70AON (AON) into cultured HS-RDEB keratinocytes and stained with an antibody against type VII collagen. Cont: no treatment of AON. Some cells were shown to express type VII collagen after the treatment (arrows).

revealed markedly reduced anchoring fibrils in the basement membrane zone (data not shown).

Rescue of type VII collagen expression in DEB keratinocytes *in vitro*

To examine *COL7A1* expression in the HS-RDEB keratinocytes treated with hm70AON, we transfected hm70AON into cultured HS-RDEB keratinocytes and stained with an antibody against type VII collagen (LH7.2). Some cells were shown to express type VII collagen (Figure 6). The rate of cell expression per total number of cells was 6.2%. We transfected h70AON1 and h70AON2, but no cells showed collagen VII immunoreactivity (data not shown).

Injection of hm70AON to the graft from DEB keratinocytes and fibroblasts

To determine the therapeutic feasibility of AON therapy in clinical practice, we constructed an artificial skin graft using HS-RDEB keratinocytes and fibroblasts, transplanted the graft to a nude rat, and then injected 30 μg of hm70AON to several portions of the graft. Saline was injected as a control. RT-PCR with the 66–72 primer set amplified only 347 bp band containing exon 70 and a weak signal for the 299 bp band without exon 70 from the treated sample (Figure 7a). The 70Δ primer set detected 305 bp band only in AON samples, indicating exon skipping of 70 (Figure 7b). Control samples did not express either 299 bp band by the 66–72 primer set, or 305 bp band using the 70Δ prime set. Furthermore, we performed immunohistochemical analysis of the treated graft with a type VII collagen antibody and could detect definite but intermittent linear dermal-epidermal junction immunoreactivity in the majority of treated samples, whereas no immunoreactivity was observed in control samples (Figure 7c and d).

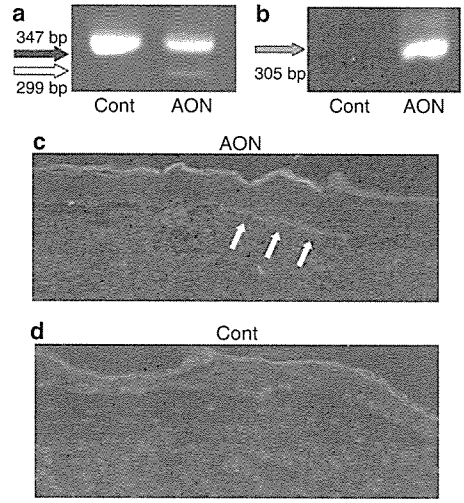

Figure 7. **Injection of hm70AON into the graft from DEB keratinocytes and fibroblasts.** We constructed an artificial skin graft using HS-RDEB keratinocytes and fibroblasts, transplanted the graft onto a nude rat, and then injected hm70AON into the graft. Saline was injected in a control. (**a**) RT-PCR with the 66–72 primer set amplified a 347 bp band containing exon 70 and a weak signal with the 299 bp band without exon 70 from the treated sample. (**b**) The 70Δ primer set detected only the 305 bp band in AON-treated samples. (**c**) Immunohistochemical analysis of the treated graft with type VII collagen antibody detected discontinuous, linear immunoreactivity along the dermal–epidermal junction (arrows). (**d**) Saline was injected in a control graft. Original magnification (**c**, **d**) × 200.

DISCUSSION

Type VII collagen, a non-fibrillar collagen, is a major component of anchoring fibril loop structures beneath the epidermal basement membrane (Uitto *et al.*, 1992; Burgeson, 1993). Cloning of collagen VII cDNA demonstrated a primary sequence of 2,944 amino acids and the basic organization of the functional domains (Christiano *et al.*, 1994a). Subsequent genomic cloning has highlighted the structural organization of the collagen VII gene (*COL7A1*) (Christiano *et al.*, 1994b).

This study has examined the feasibility of targeted exon skipping using AON. As the intron/exon organization of *COL7A1* contained 118 multiple short exons, deletion of one shorter exon may not significantly interfere with type VII collagen function. In fact, a mutation study revealed that several *COL7A1* splice-site mutations causing skipping of one exon resulted in a milder phenotype than the expected HS-RDEB that harbors nonsense mutations causing a lack of *COL7A1* expression (Terracina *et al.*, 1998). Furthermore, DEB mutations were frequently found in exons encoding collagenous domains and the nucleotide number of these exons is definite multiples of 3. This indicated that abolishment of exons restored an open leading flame of *COL7A1*. These characteristic features of the gene structure encouraged the start of research into the possibility of AON skipping therapy.

COL7A1 mutation database demonstrates presence of recurrent *COL7A1* mutation, and AONs, which are suitable for recurrent mutation, of course, are applicable for more patients than AONs for rare mutation. Thus, this study targeted exon 70 AON therapy, as the recurrent premature termination codon mutation 5818delC in exon 70 was found in more than 20% of recessive DEB sufferers (Tamai *et al.*, 1999; Sawamura *et al.*, 2005). We first synthesized two potential AONs, h70AON1 and h70AON2, for exon 70 and the results indicated that h70AON2 was able to induce skipping of exon 70 *in vitro* and *in vivo*. To understand the effect of exon 70 deletion on the essential functions of type VII collagen, we constructed *COL7A1* cDNA without exon 70 (*COL7A1*Δ70) and introduced this defective gene to HS-RDEB *in vitro* and *in vivo*. The results of attachment and migration analyses showed that the deleted collagen had an apparently similar function to the normal collagen. Next, we examined the ability of the defective collagen to form anchoring fibrils. To eliminate internal expression of type VII collagen, we used keratinocytes and fibroblasts from HS-RDEB who exhibited no *COL7A1* expression and failed to form any anchoring fibril-like structures in patient skin. Ultrastructural examination of the skin graft treated with *COL7A1*Δ70 demonstrated anchoring fibril formations in the sublamina densa. These results indicate that type VII collagen, lacking the 16 amino-acid sequences from exon 70, exhibits a remarkably near-normal assay similar to the normal type VII collagen.

As the sequence of h70AON2 was located at the 5818delC mutation site, we synthesized a mutation-specific AON hm70AON to match the sequence with deletion of 5818 cytosine. After transfection of hm70AON into HS-RDEB harboring the 5818delC defect, RT-PCR demonstrated effective exon 70 skipping. However, as predicted, when this AON was introduced to normal human keratinocytes, we found little skipping against exon 70 in the wild *COL7A1* allele. Some recessive DEB patients harbor heterozygous mutations 5818deC and missense mutations, which would not interfere with the function of this type VII collagen. In this case, hm70AON benefited by not altering the expression of *COL7A1* on the other allele. Further immunofluorescence studies using HS-RDEB cell culture systems showed that transfection of hm70AON could rescue type VII collagen expression in patient's keratinocytes. Approximately, 6% cells began to synthesize type VII collagen.

Finally, we constructed artificial HS-RDEB skin from the patient's keratinocytes and fibroblasts, and introduced hm70AON to the graft. RT-PCR analysis using the 66–72 primer set and the 70*Δ* primer set detected the presence of exon 70 skipping in the treated graft. Furthermore, immunofluorescence using type VII antibody demonstrated the positive expression of type VII collagen along restricted parts of the dermal–epidermal junction. Although we obtained the samples from several specimens and carried out electron microscopic analysis, we could not observe obvious anchoring fibrils ultrastructurally. We might examine no section corresponding to the restricted immunoreactive parts.

We recently suggested that fibroblasts might be a better gene therapy target of DEB treatment than keratinocytes (Goto *et al.*, 2006). The majority of collagen VII *in vivo* are thought to originate from keratinocytes because the level of *COL7A1* expression in the epidermis was much higher than that in the dermis. However, when *COL7A1* expressions of keratinocytes and fibroblast were almost equal after retroviral transfer of *COL7A1*, the gene-transferred fibroblasts supplied a higher amount of collagen VII to the new dermal–epidermal junction than the gene-transferred keratinocytes (Goto *et al.*, 2006). The AON therapy cannot generate an additional *COL7A1* expression, and it just modifies the existing expression. So, we think that AON transferred into keratinocytes gives predominant therapeutic effect in this study.

Finally, disadvantages of this AON approach for DEB are proposed. First, the effect disappeared immediately because AON is easily degraded in the cells. This study showed that the effect of AON was totally extinct 72 hours after the transfer of AON *in vitro*. Second, the method cannot induce the perfect full-length collagen VII. There is the possibility that in-frame exon skipping may lead to a dominant-negative interference. In fact, a 16-bp internal deletion in the *COL7A1* gene leading to in-frame exon skipping caused dominant phonotype of DEB (Cserhalmi-Friedman *et al.*, 1998). Third, transfer efficacy of AON to the skin is relatively low. Kinetic analysis of oligonucleotide topically applied to mouse skin showed early follicular localization, diffusion of the oligonucleotide from the mid-follicle, and subsequent dermal accumulation (Dokka *et al.*, 2005). Our study transfer efficacy was low in our skin graft experiment, but application of AON to actual skin may show a higher transfer efficacy, perhaps owing to the increased presence of skin appendages. In conclusion, we believe that improvement of these points enables this strategy to be applicable to clinical practice.

MATERIALS AND METHODS

AON

We selected exon 70 for AON therapy as the recurrent premature termination codon mutation 5818delC was present in exon 70 in DEB patients (Tamai *et al.*, 1999; Sawamura *et al.*, 2005). We designed a potential AON for exon skipping using the RNA mfold version 3.1 server (Zuker, 2003), and synthesized a full-length phosphorothioate backbone and HPLC-purified 2′-*O*-methyl-modified ribose